+Modern Laser Peening for Material Surface Enhancement

Micheal A. Kattoura, Stanley C. Bovid, David F. Lahrman, and Allan H. Clauer

1. Introduction

Laser peening, or laser shock peening, is a surface enhancement process that relies upon shockwave mechanics to generate large magnitude, deep residual compressive stresses in materials. The effects of laser peening are routinely observed at depths up to ten times deeper than conventional peening technologies. The improvements of material properties are derived from the superposition of stress states (residual and applied).

Laser peening is currently used in several industries to combat various metal failures in variety of alloys. In aviation, laser peening is used to enhance resistance against Foreign Object Damage (FOD) of titanium blades, also to enhance resistance to fatigue and stress corrosion cracking of aluminum structures. In the power generation industry, laser peening is used to enhance the fatigue loading, fretting fatigue and contact fatigue properties of steel components. In the chemical and nuclear industries, laser peening is preventing stress corrosion cracking of nickel-based alloys and stainless steels. In the shipbuilding industries, laser peening is combating stress corrosion cracking of aluminum ship hauls operating in open sea saltwater. In manufacturing, laser peening is enhancing the life of various components such as pilger dies, casting dies, cutting blades, crankshafts, and other structural components manufactured from variety of metals and experiencing various metal failures.

The process has been in existence for over 50 years and has been used in commercial production since the 1990's. Improvements in the laser equipment technology that drive laser peening have hardened the process and increased throughput rates over the last 30 years. This combination of events has dramatically reduced costs and thereby enabled laser peening as a viable commercial process for many industries.

The vast benefits of the process continue to generate attention worldwide, both in industry and in academic research. The sustained growth and interest in laser peening from both sectors of development continues to raise awareness of the process and develop tools to reduce cost and enable new markets.

This chapter provides an overview of the laser peening process and its material enhancement capabilities. In addition, the chapter presents the latest advancement in the technology that are enabling its growth to various on-site applications and expansion to different industries.

2. Brief Historical Overview

The process of laser peening has been in development for nearly as long as laser technology itself has been available. The physical effects of pulsed laser interaction with materials was first reported in the late 1960's and early 1970's [1–5]. The first observation of plastic deformation in metals by laser-induced shock wave was observed at Moscow State University in 1970. In 1974, the use of lasers to improve properties by inducing shockwaves was patented by Mallozzi and Fairand [6]. Throughout the 1970's and early 1980's, the characteristics of the laser-materials interaction and the material response to the induced shock waves were further investigated [7–12]. These early developments of the technology helped form the fundamental basics for modern, commercial laser peening practices.

Despite the significant developments during this time period, implementation of the technology was severely limited by the processing rate of laser systems available. The high cost and slow processing rate, approximately 1 pulse every 8 minutes, prevented laser peening from gaining acceptance as a viable surface enhancement process for many years. During the

late 1980's laser technology reached a development stage that enabled the process for industrial use. It was during this time period that the process became known as laser peening and was used to enhance the fatigue life of metal parts [13]. Outside of industrial development, academic pursuit of a deeper understanding of the physics of the process and broader investigation of its effect on material properties also occurred [14,15].

In the mid 1990's, the first industry-oriented project for laser peening involved the processing of aircraft gas turbine fan blades for increased foreign object damage resistance [16]. This first industrial project also led to the formation of the first company to provide laser peening equipment and services in 1995, LSP Technologies, Inc.

Due to the cost of the process during the growth stages of the technology, the laser peening process remained generally confined to application on high dollar, high risk parts. In the U.S., funding from government institutions and industry helped mature the process and equipment and reduce the cost in the early 2000's. This government interest enabled new applications in many industries where the residual stresses imparted by other surface enhancement processes were insufficient or undesirable.

In Japan in the early 1990s, Toshiba began developing a laser peening system entirely different from the high energy pulsed lasers being used at that time in the USA and Europe [17]. The system was specifically developed to treat structural features inside water-filled boiling water reactors (BWR) and pressurized water reactors (PWR) to mitigate stress corrosion cracking problems [18].

On the research side, several groups around the world were conducting research in parallel to the early industrial applications. Clauer [18] lists some of the earliest research groups. In France, starting from the mid of 1980s into 1990s, Fabbro, Peyre and colleagues conducted an extensive, broadly-based program in laser peening centered around their high energy pulsed laser facilities. The French programs have made an important and significant contribution to advancing the understanding of laser shock processing to where it stands today. In China, starting from 1996 several research groups investigated laser induced shock such as Zhiyong Li and colleagues at University of Science and Technology in Hefei, Yongkang Zhang at Nanjing University and Yongkang Zhang and Jianzhong Zhou at Jiangsu University. In Spain, in the late 1990s, Professor José Ocaña and colleagues at the Universidad Politécnica de Madrid, began developing a comprehensive model for laser shock processing. In the early 2000s they initiated an experimental program. Ocaña and his colleagues have contributed significantly to the understanding of laser processing technology over the last 20 years. As of 2021, several commercial facilities are providing production laser peening services and multiple research and academic institutions around the world continue to provide important research contributions. Commercially available laser peening equipment is also offered for sale and lease by select companies.

The growth of the laser peening industry is expected to continue as the technology becomes even more hardened and industrialized. Evidence of this growth can be seen by the increased number of laser peening facilities, quantity of production components being laser peened, continued participation and expansion of the international conferences on laser peening, increased technical paper publication volume, and the growing number of worldwide patents related to the process.

3. Process Overview
Many specific details related to the process of applying laser peening are unpublished and are often considered to be trade secrets. Regardless of supplier specific procedures related to laser peening, the underlying physics of the process remain the same. Laser peening is a mechanical

process that is initiated by a thermal event. In most industrial applications, the surface of a component being treated does not see any appreciable change in temperature from ambient.

Traditional laser peening requires only two components: a high-powered pulsed laser and a transparent overlay. Other components are frequently implemented to enhance the processing effects; however, they are not necessary for the fundamental process to occur. During processing, the target surface is covered with the transparent overlay. The transparency refers to the transparency of the overlay to the laser beam; that is, the laser beam passes through the overlay without an appreciable absorption of energy. The high-power laser beam passes through the transparent overlay and strikes the target surface. This initial material interaction vaporizes a thin layer of the target and creates a small cloud of vaporized material. With continued delivery of laser energy, the vaporized material is rapidly heated and converted into plasma. This plasma is confined by the transparent overlay, typical water, which causes the pressure within the plasma to rise rapidly. The rapid pressure spike initiates the shockwave to propagate into the surface of the target. Typically, the pressure pulse from the plasma expansion is about 2 – 3 times the duration of the laser pulse [8].

In most processing scenarios, the transparent overlay is used to act as a tamping layer to the plasma, confining it to increase the peak pressure generated by the plasma expansion. Without the transparent overlay, the plasma is not contained and the peak pressure is typically insufficient to generate a shockwave with enough intensity to modify the mechanical properties of the target. The shockwave from a confined plasma causes dynamic yielding in the material when the shockwave pressure is above the dynamic yield strength of the material which is referred to as the Hugoniot Elastic Limit (HEL). Most metallic engineering alloys have HEL values in the 0.5 – 4 GPa range. As the shockwave propagates into the material, the wave attenuates and the peak pressure decays. When the shockwave pressure is below the HEL the wave essentially becomes an elastic stress wave and does no further work. By passing through previously shocked locations, iterations of processing the same area allow each subsequent shockwave to propagate to deeper depths with higher stress magnitudes.

The initial vaporization of the target material dictates that a superficial amount of the surface is atomized during the process. The plasma creation also generates intense temperature increases that are of very short duration (nanosecond scale). These rapidly occurring events can lead to superficial melting and staining of the part surface if it is not protected. The staining is typically a result of oxidation products generated during the process. These stained locations also can exhibit superficial tensile residual stresses from the thermal effects on the material. This basic method of laser peening is often referred to as bare surface processing or in some cases, Laser Peening without Coating (LPwC).

Due to the advancement of laser technology, the power of peening systems have drastically increased over the past decades, significantly increasing processing rates and reducing processing costs. Bare peening (no opaque overlay) has become a predominant processing method for economical, process efficiency and throughput reasons. In addition, there are scenarios that applying protective layer is not possible such as processing of components underwater or in geometries with limited access. For example, in the inside of in-service nuclear reactor cooling systems, it is impractical to use an opaque overlay. Through a combination of small spots and short pulse lengths, bare laser peening can be accomplished on these reactor walls [19,20].

Some commercial laser peening is still being performed using an opaque overlay as a surface protectant especially when processing Titanium alloys. The use of opaque overlays provides some benefits over bare surface processing for some alloys: vaporization of the opaque overlay protects the target material surface from direct laser beam and thermal interaction; and the overlay can increase the transmitted shock pressure and prevent melting and oxidation of

surrounding material. A diagram of the laser peening process with opaque overlay is shown in Figure 1.
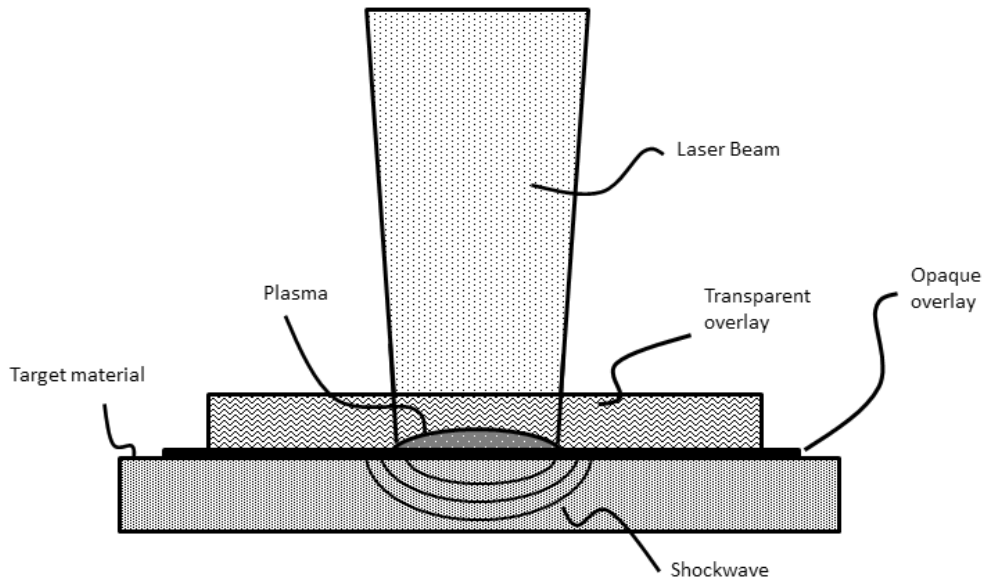

Figure 1. Schematic of the laser peening process showing the overlays in place and the laser beam irradiating the material surface. The image is not drawn to relative scale.

4. Laser Peening Parameters

The subsections that follow discuss generic processing effects resulting from the various laser peening parameters. These are meant as guidelines to be considered in processing configurations. Specific examples of the key parameter variation and resulting material data are provided in Section 5.1.2, Residual Stress Manipulation Through Processing Conditions.

4.1 Intensity and Coverage

Laser peening parameters are not currently standardized across the industry and variation exists depending on specific system capabilities. To minimize the differences and specifics from multiple laser system, the process can be broken out into several main components to maintain relative details from one system to another. Important characteristics that must be considered for the process are: the energy delivered per pulse (E, in joules, J), the full-width half-max (FWHM) pulse duration (pulse width, pw, in nanoseconds, ns), the spot size of the laser beam on target (area, A, in cm^2), and finally the coverage which is the number and distribution of laser pulses used for processing which is commonly referred to in the industry as the number of times or layers that a given surface is processed (coverage, in layers). As a general guideline, specification of the process is frequently based on the power density (Pd, in GW/cm^2), which incorporates the laser energy, pulse width, and spot size into a single value. The power density refers to the amount of energy that is delivered over a specified time frame in a given area by the laser beam. In equation form, this can be calculated as:

$$Pd(\frac{GW}{cm^2}) = \frac{E(J)}{pw(ns) \times A(cm^2)}$$

The duration of the laser pulse is an important parameter for the laser shocking process. Longer duration pulses sustain the plasma expansion for longer periods of time. In turn, the resulting shockwave duration is longer and penetrates deeper into the material. Laser pulse duration (pulse width) is frequently in the 8 – 25 ns range for laser peening. As noted earlier, the effective length of the resulting pressure pulse is typically 2 – 3 times the length of the laser pulse and is used as means to control the residual stress profile.

Coverage of the surface can be specified via several different means depending on laser system capabilities. Laser peening is carried out by the application of sequential laser beam pulses on a surface to be treated. Essentially, each laser beam pulse is assigned a geometric position of interaction with the target. Typical industrial laser peening coverage is achieved by applying laser spots in a sequential series. However, coverage can also be performed by simultaneous processing of areas. This may be on the same face of a component or opposed faces. The coverage may be defined as percentage of overlapped laser beam shots (%), number of layers of coverage (layers), or in pulse density (pulses/cm^2). Industrial laser peening practice has shown that residual compressive stresses are generally increased in both magnitude and depth with increasing coverage. A depiction of how laser peening coverage may be applied to a turbine airfoil is shown in Figure 2. Later sections (Section 4.3, Laser Systems) of this chapter focus on several differences between laser systems that necessitate the variation in coverage terminology and practice, particularly for small spot laser peening technology.
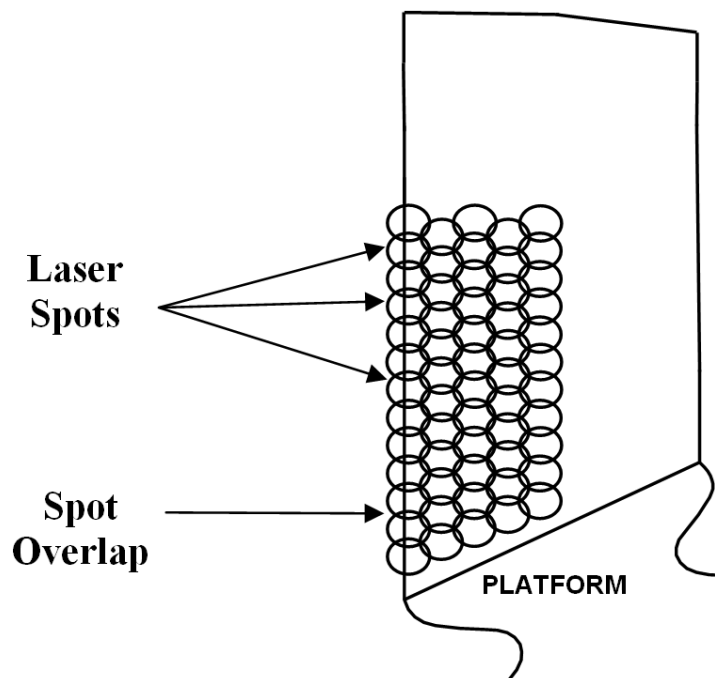

Figure 2. Depiction of laser peening patch that may be applied to a turbine airfoil.

An example of a laser peening processing condition that is commonly used for titanium alloys is: 9 GW/cm^2, 20 ns, 3 layers and is sometimes displayed in a simple form as 9-20-3. The complete range of optimal processing conditions (power density, pulse width, coverage, spot size, overlays, etc.) is rarely found in publications, and technical expertise of commercial organizations is usually relied on for the selection of optimal parameters.

4.2 Transparent and Opaque Overlays

Laser peening process requires the use of a transparent layer that helps confine the plasma and generate the shockwave into the material. An opaque overlay is an optional layer that can help amplify the magnitude of the shockwave and protect the surface of the material from interacting with the plasma.

The most common transparent overlay used in laser peening is water. Water is readily available, inexpensive, and provides a self-renewing coverage of the part surface. Typically, the part can be immersed in water or it can be flowing over the surface to conform to the surface geometry. Typically, the transparent overlay has a thickness of 0.5 – 1 mm. This thickness provides sufficient confinement of the plasma for the few hundred nanoseconds which is sufficient to generate the shockwave into the material. Other transparent overlays that have been used in

research include transparent tapes, transparent gels, solid overlays of glass, fused quartz and acrylic [12]. The tradeoffs of performance and efficiency of these other overlays have not presently justified their use in production laser peening.

While the majority of laser beam energy passes through the transparent overlay (approximately 97% at 1 mm of water), there is a limit to the power density that can be passed. For systems with wavelength around 1054 nm, at high power density levels, in the vicinity of 12 GW/cm^2 for water, di-electric breakdown occurs. The di-electric breakdown limits the amount of laser beam energy that reaches the target surface and can prevent optimal processing. For this reason, the target power density is typically limited to a maximum of 10 GW/cm^2. This limit changes for laser peening systems utilizing different wavelength [21].

In applications that require opaque overlay, there are several considerations when selecting an opaque overlay. Those that affect the cost and control of the process include: the ease of application and removal from the material surface, ability to maintain coating integrity for multiple shots and over complex surface geometries, disposal of used overlay material, and repeatability. Those that affect the shockwave characteristics are thickness, laser interaction response and acoustic impedance. Due to the time requirements for utilizing opaque overlays and the complexity of applying for several applications, industrial laser peening is moving away from utilizing opaque overlays except for components that require protection from the plasma interaction (mainly Titanium components).

The selection of materials that can be used for the opaque overlay is fairly broad, provided the material absorbs the laser beam energy. Paint, vinyl and metallic tapes, foils, and proprietary formulations of products are the most commonly found overlays. The overlays are kept thin to minimize pressure loss in transmission but require sufficient thickness to prevent thermal effects from reaching the base metal. The short duration of the plasma requires only that approximately 1 - 30 μm of opaque overlay be used but is dependent on the specific overlay type. In most cases, the laser peening process will partially obliterate the opaque overlay at the target location. This may require that multiple applications of the overlay be performed during a processing cycle to protect the part surface if the overlay is not self-renewing.

4.3 Laser Systems
Laser peening can be accomplished via the use of a wide range of pulsed laser systems. There are typically tradeoffs between each laser system in terms of costs, laser footprint, maximum benefits obtainable, and throughput. The different pulsed laser systems used for laser peening are generally classified into two groups: 1) Higher energy, lower pulse frequency lasers; and 2), lower energy, higher pulse frequency lasers. Table 1 below highlights some of the differentiation between the groups.

Historical industrial application of the laser peening process in the United States and some research groups around the world utilized lasers with very high energy up to 50 Joules but very low pulse frequency < 1Hz. The early systems used were for example a 90 J, 20 ns at Laboratoire d'Application des Lasers de Puissance (LALP) in Arcueil, France [22]; a 50 J, 20 ns at 0.5 Hz Battelle and LSP Technologies Inc. (LSPT) legacy lasers and GEAE Gen1 [18]. With further development of the laser systems, these companies switched towards lower energies up to 20 J and intermediate frequency up to 20 Hz to achieve higher throughput and decrease the equipment costs. Examples of these systems are 10 J, 20 ns at 10 Hz GEAE Gen4 and University of Cincinnati; 10 J, 8 – 20 ns at 20 Hz LSPT's Procudo® 200 Laser Peening System [23]. The initial systems consisted generally of a pulsed Nd:glass laser with wavelengths on the order of 1054 nm. Some systems combine glass rods and slabs [24]. The newer systems being used today by LSPT and others utilizes Nd:YAG and Nd:YLF lasers. The pulse lengths are generally within the range of 6 to 40 ns, with the majority of industrial work performed in the range of 8 to 25 ns. This group is denoted as Group 1 in the summary Table 1.

On the other hand, initial industrial systems used in Japan utilized low power Nd:YAG lasers operating at higher frequencies, shorter pulse durations and in the 532 nm range. Lower power laser systems often operate at less than 1 Joule per pulse and require small spot sizes to achieve the desired laser beam power density required for laser peening [19,20,25]. Examples of these systems are 60 - 100 mJ with 5 ns at 120 Hz Toshiba for nuclear industry [26]. LSPT's Procudo® 60 and Procudo® 140 utilize lasers in the hundreds of mJ and frequency up to 200 Hz. Several research groups utilize laser systems of few joules and frequency up to 10 Hz since they are the cheaper, smaller and easier to handle. One of the first uses of such laser peening system is a 2J 10 Hz at the Universidad Politécnica de Madrid [18]. Similar systems can be found at University of Texas at Dallas, University of Nebraska at Lincoln, and University of Cincinnati.

Table 1 Groupings of different laser systems by capabilities.

Group	Energy (J)	Frequency (Hz)	Spot Size (mm)
1	5- 50	0.1 - 20	2 - 7
2	0.01 - 5	10 - 200	0.25 - 1

The availability of laser systems from these two vastly different groups provides the flexibility needed for designing laser peening systems that are tailored to address specific challenges in large array of industries. Explanation of how these systems are incorporated with various beam delivery solutions to support different applications is presented in section 4.4. In addition, investigations of laser systems outside of the two above groups are being conducted and an example of such a system is presented in section 8.4.

Moreover, laser peening companies are utilizing the improvements in the laser technology to enhance the durability, reliability and robustness of the laser systems while decreasing the size of the lasers and reducing maintenance. A major advancement in the laser technology implemented in laser peening systems is diode-pumped lasers that are replacing the flashlamp lasers. The diode-pumped lasers provide orders of magnitude increased life of the system before the need for maintenance. In addition, advancement in the laser components, optical components and layout designs are allowing for compact table-sized systems compared to the older room-sized systems.

4.4 Beam Delivery

The beam delivery design is customized for the intended application of the laser peening system. The two approaches for the beam delivery are fixed-beam and moving-beam delivery. The fixed-beam delivery is used for application where you can move the part and have a line-of-sight to the processing areas. Moving-beam delivery is used for applications where the part is too large to be moved or for applications where the processing areas are hard-to-see or internal.

Each of these beam delivery options can utilize laser systems from either group described in section 4.3 based on the application. To support the vast array of industries and applications, having capabilities that stretches in all categories provide flexibility in designing laser peening systems and optimizing the performance enhancement and throughput requirements. Companies such as LSPT utilize systems from all groups to meet customer's requirements.

4.4.1 Fixed-Beam Laser Peening Equipment

Typically, the laser beam is brought to a fixed point in the processing cell and robots are used to position the part at the desired location relative to the laser beam to laser peen the specific location. The part can then be moved through the laser beam to achieve the desired area of processing.

These systems can be used as a job-shop setup that allows provides flexibility that allows processing of various types of components. Advancement in laser systems has reduced the cost, footprint and maintenance while improving the robustness of these systems to be incorporated in manufacturing production lines. This allowed designing application-specific laser peening systems that utilize specialized part handling tools designed for the optimum processing of the components.

An example of fixed-beam laser peening equipment is the Procudo® 200 Laser Peening System used for application development and production processing at LSPT shown in Figure 3 and Figure 4. This system can deliver two separate laser beams to the processing cell. The beams go from the laser system, Figure 3, through the wall, into the processing cell, as shown in Figure 4. The laser can be configured for either single or dual beam processing of 10 J total energy. In the processing cell, the laser beams are contained within enclosures on the beam tables and pass through the beam delivery tubes. The beams are stationary during processing, and the robot shown in Figure 4 manipulates the part being processed through the laser beam path during processing. A 6-axis robot is used to provide the flexibility needed for developing laser peening for a variety of parts, and for small production runs of different parts. For high volume production runs requiring high throughput, a parts-handling machine tool specifically designed to minimize the time required to insert and remove a part for processing can replace the robot. In addition, advancements in robotics programming are incorporated to minimize cell downtime for setting up new parts. Offline programming provides the ability to program new parts on software that mimics the laser peening cell and allows quick setup of new parts.

Figure 3. Procudo® 200 Laser Peening System showing laser system, with a processing cell shown in Figure 4.

Figure 4. Processing cell for Procudo® 200 Laser Peening System showing beam delivery tables and the robot for manipulating parts during processing. The laser system is on the other side of the wall behind the cabinets.

4.4.2 Moving-Beam Laser Peening Equipment

When working with components that are too large to move or components with areas that are hard to reach, there is a need for laser peening equipment that brings the laser beam to a stationary component such as an aircraft, ship, nuclear reactor, and other fixed structures. There are different approaches that have been implemented to bring the laser beam to the part.

4.4.2.1 Mirrors and Beam Tubes

One of the earliest applications to bring the laser peening to the component was Toshiba laser peening nuclear reactor components. The development of the system started in 1993 and the first industrial application was performed in 1999 [27]. The design utilizes mirrors and beam tubes that contain mirrors within pipes with flexible joints to allow for movement of the end effector such as the rotating cart shown in Figure 5 (a). This system was able to deliver the laser beam underwater to the optimum location for laser peening with full monitoring of the process. The laser peening system utilized a group 2 low energy laser system with green wavelength (around 532 nm).
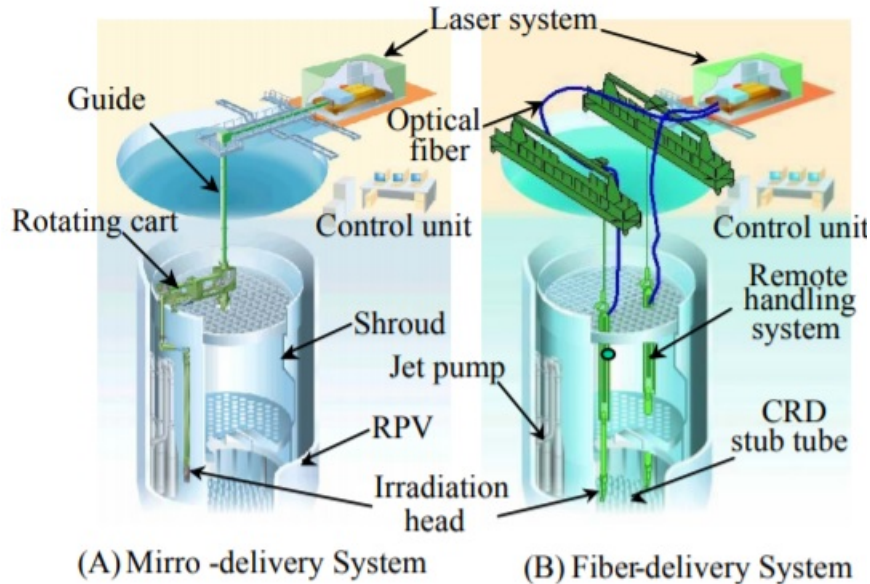
Figure 5: Toshiba moving beam laser peening equipment: (A) Mirror delivery system; (B) Fiber delivery system. After [28].

4.4.2.2 Articulated Arm:

A further advancement of the previous design was developed by LSPT. This system utilizes an articulated arm which contains mirrors on each joint of the arm to deliver the beam to hard-to-reach locations. The articulated arm provides higher degrees of freedom for controlling the positioning of the laser peening process. Examples of applications that can utilize this beam delivery are chemical plants and nuclear plants fixed components in addition to large structures such as large ships for shipyard applications. The system is designed to utilize a group 1 high energy laser system operated in air environment. Figure 6 shows the main features of the articulated arm laser peening system developed by LSPT.
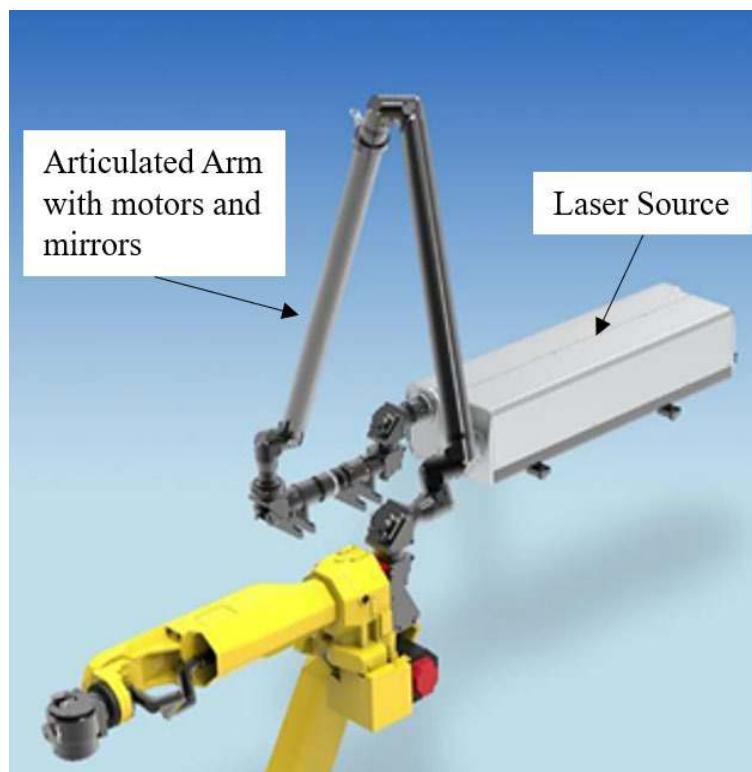
Figure 6: LSPT articulated arm laser peening equipment.

4.4.2.3 Fiber Optic with Specialized Tooling

10

Another approach to delivering the laser beam to a target is with fiber optics. Fiber optic can carry the laser beam energy far distances to a laser peening tool to conduct laser peening in a specific location on a component as shown in Figure 5 (b). The fiber optic provides high maneuverability and ability to laser peen hard to reach small compartment areas. On the other side, there is limited allowable energy that can be carried by a single fiber. These laser peening systems generally utilize group 2 laser systems. Fiber bundle extends the capabilities of such laser peening systems to higher energies allowing utilization of group 1 laser systems. The earliest application of this technology was done by Toshiba for nuclear applications. The development of the system started in 1998 and the first industrial application took place in 2002 [26,27]. In 2018, LSPT announced the development of fiber optic delivered and custom tools laser peening system to carry miniaturized laser peening technology to mission-critical components [29]. Examples of applications that can utilize this beam delivery is tight compartments such as in aviation. In addition, the fiber optic provided added flexibility for manufacturing integrated systems.

4.4.2.4 Portable Laser Peening (PLP) System
Due to advancement in the size of the lasers, Toshiba designed a laser peening system that incorporates the laser system as part of the processing tool that reduces or eliminates the need for articulated arms and fiber optics [27,28]. Figure 7 shows the laser peening equipment that contains the laser source in close proximity of the part. This laser system is connected to an umbilical that supplies power, cooling water and controls from the operation floor. This laser peening system was designed for underwater nuclear applications.
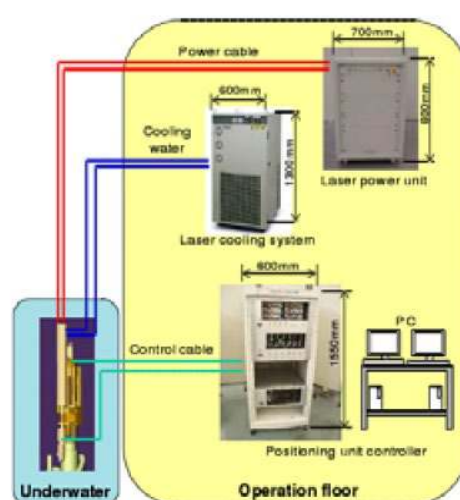

Figure 7: *Portable Laser Peening (PLP) System. Per* **[28].**

4.4.2.5 Handheld equipment
A further technology development allows for a potential reduction on the size of the laser source that could promote the design of small palm size system to promote unique applications of laser peening. These Palmtop Lasers were developed by Professor Sano and coworkers [30]. Figure 8 shows an image of the ultra-compact 20 mJ prototype of the palmtop laser. This laser peening system is very light and compact and can be the solution for onsite localized treatment and repair processes similar to the handheld ultrasonic peening devices commonly used in bridge repairs on welded areas [31].
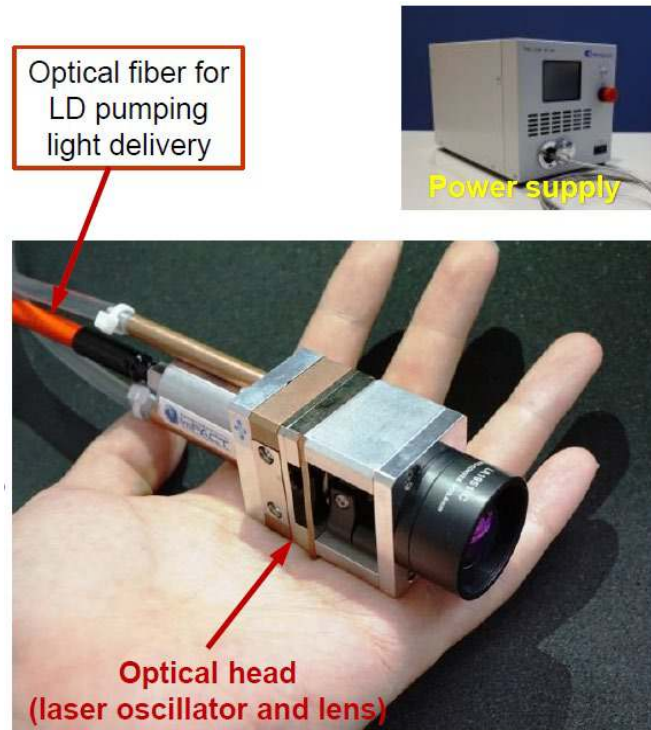
Figure 8: Prototype of palmtop laser (20 mJ system). Per [30].

5. Laser Peening Effects on Material Properties

5.1 Residual Stresses

The improvement of material properties via laser peening is the result of residual compressive stresses formation at the surface to mitigate surface-initiated fatigue. For laser peening, the residual compressive stresses have been observed at depths greater than 8 mm deep in particular applications; however, the typical depth of treatment is between 0.75 mm to 2 mm for components with thickness greater than 5 mm. For reference purposes, the depth of the residual stresses from conventional shot peening is typically 0.25 mm or less as shown in Figure 5. In thin sections (less than 5 mm thick), laser peening will generate through-thickness residual compressive stresses by processing of opposing sides of the component such as in turbine airfoils.

5.1.1 Residual Stress in Specific Engineering Alloys

A comparison of the difference in the residual stresses generated by laser peening and shot peening for two titanium alloys is shown in Figure 9. For both alloys, laser peening was able to achieve comparative or better maximum residual stresses near the surface and superior depth of residual stresses. The laser peening processes maintained high compressive stresses even after 1 mm depth whereas shot peening depth of treatment was around 0.25 mm. The residual compressive stresses as a function of depth for two additional engineering alloys are shown in Figure 10 and Figure 11. The residual stress after laser peening 2024-T3 aluminum, an alloy typically used in aircraft skin structures, is shown in Figure 10 [12]. The response of a high strength steel, such as AF 1410 used in landing gear applications, to laser peening is shown in Figure 11. These materials serve to illustrate the wide applicability of laser peening to produce deep residual compressive stresses in a variety of alloys.
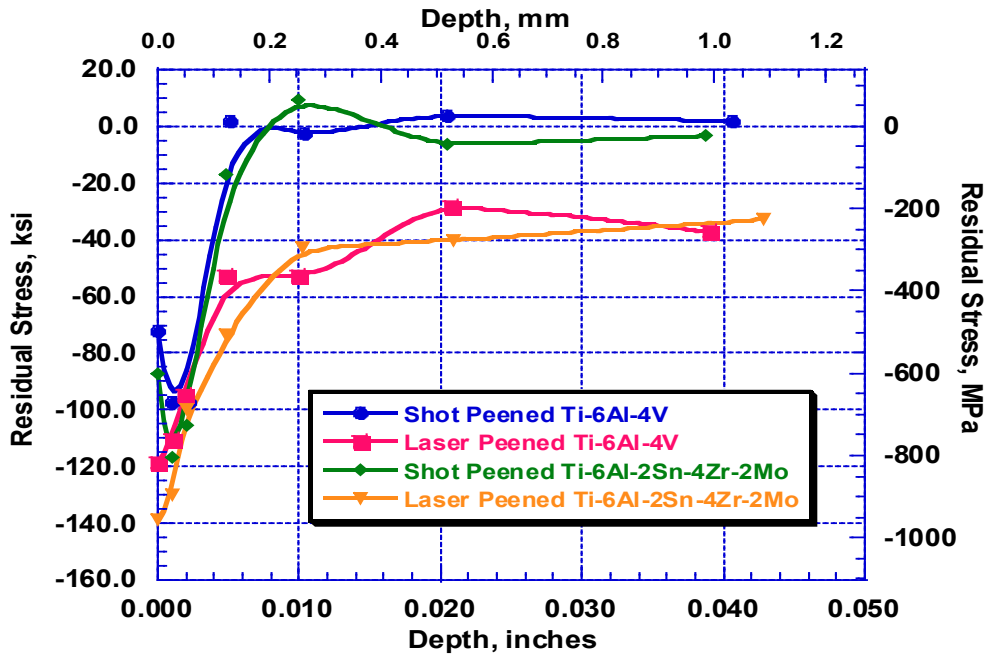
Figure 9. Comparison of residual stress profiles between laser peening and shot peening in two titanium alloys.
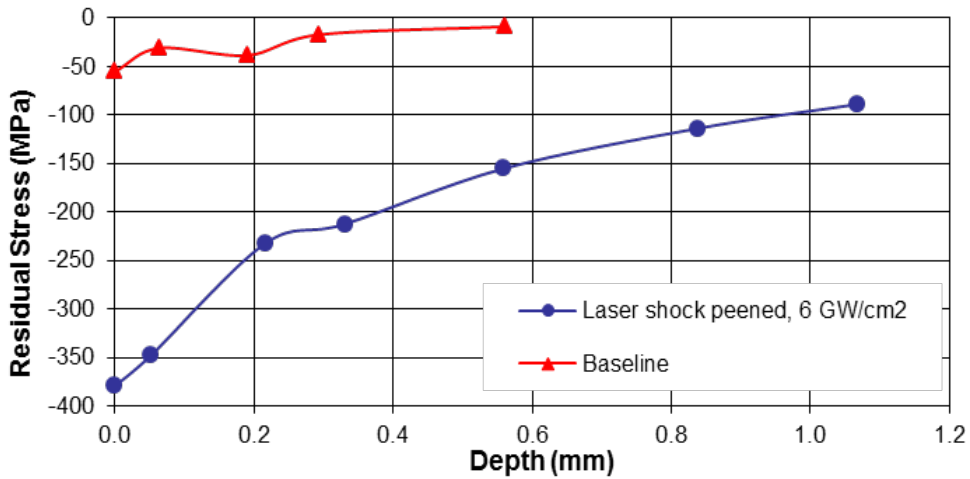

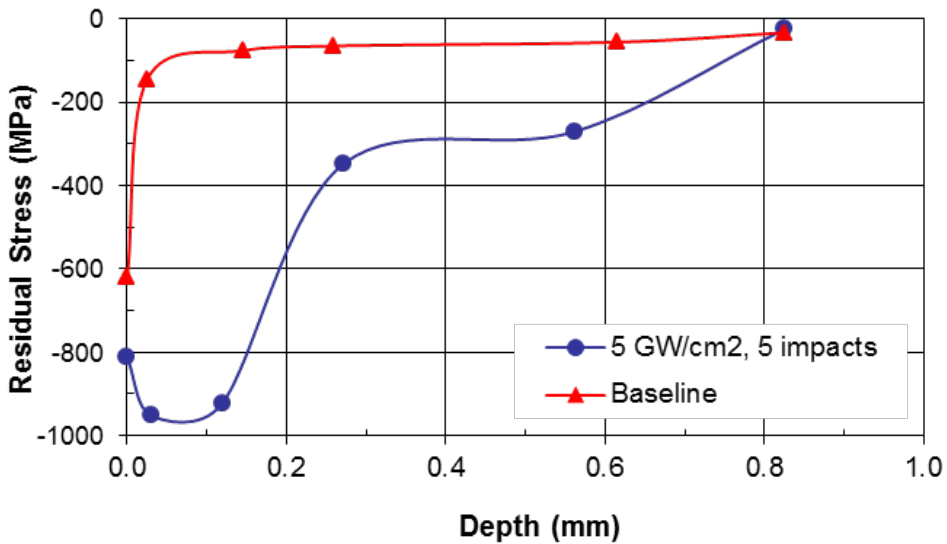**Figure 10. Laser shock peened residual stress profile for 2024-T3 aluminum. After [22].**

Figure 11. Laser shock peened residual stress profile for a high strength steel, AF1410.

5.1.2 Residual Stress Manipulation Through Processing Conditions

As highlighted in the earlier sections of this chapter, the selection of processing parameters can have a significant impact on the residual stress results. The majority of processing magnitude is controlled by the intensity and coverage (number of layers). The effect of increasing power density is shown in Figure 12 for Ti-6Al-4V. The compressive stress on the surface increases with increasing laser peening intensity, from -100 MPa for the low intensity to -650 MPa for the high intensity. In addition, the depth of the residual stresses also increases with increasing laser peening intensity. This is a result of the peak pressure remaining above the HEL of the material for more depth. As routinely observed and exemplified in this figure, the deepest compressive stresses are achieved at the highest laser peening intensity.
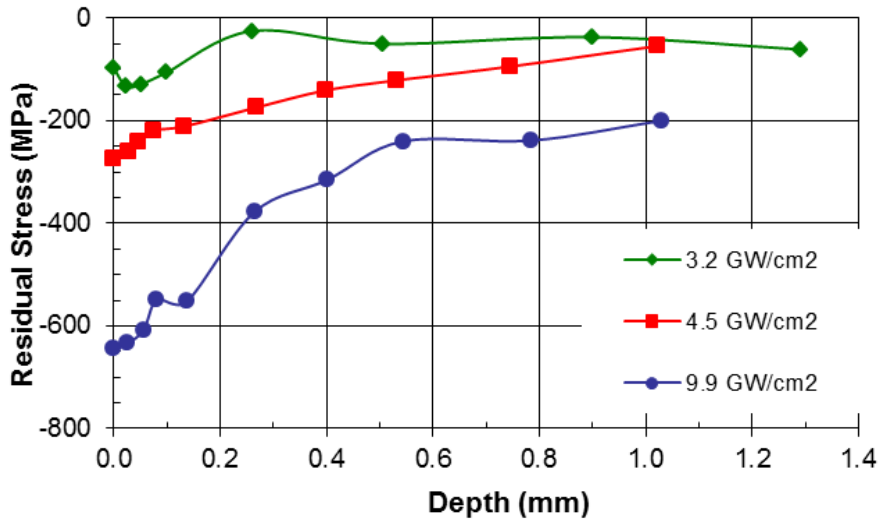

Figure 12. Residual stress profiles for Ti-6Al-4V at increasing irradiances, one impact.

As for the coverage, Figure 13 (a) shows the effect of increasing the number of layers at 2 GW/cm^2 power density on thick Ti-6Al-4V. With the increase of number of layers, there is an increase of both the surface compressive stress and depth of compressive stress (zero crossing) [33]. Figure 13 (b) shows a more detailed effect of the number of layers on the depth of residual stresses for different power densities. This figure also illustrated the benefit for increasing the number of layers from 2 to 4, but there is diminished benefit for going to a higher number of layers (8 layers at 2 GW/cm^2), considering the large increase in processing time.
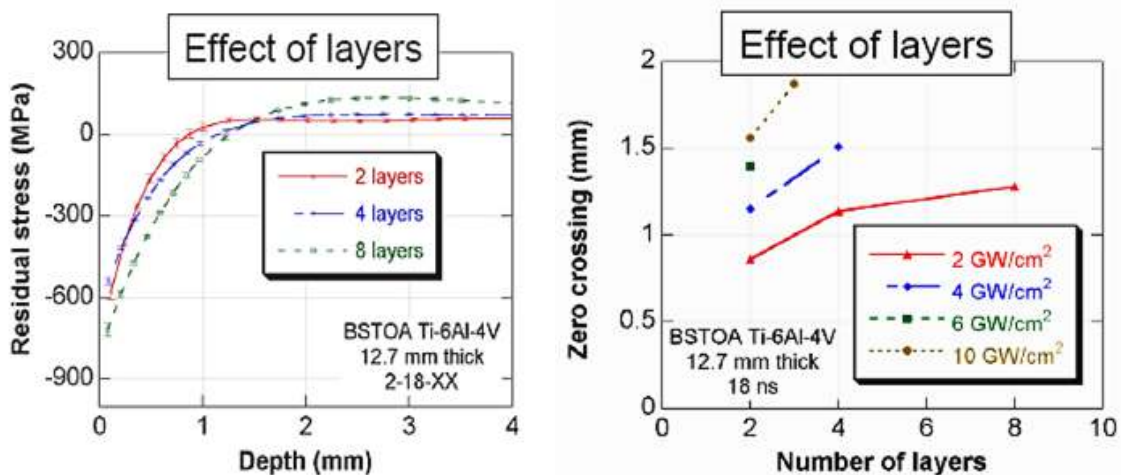

Figure 13: Effect of number of layer on the residual stress profile in Ti-6Al-4V. Per [33].

There are numerous applications, such as in fan and compressor blades in gas turbine engines, for which the area to be laser peened consists of a thin section. In this case, the airfoils areas to be

14

treated which are typically the leading and trailing edges are processed on opposite sides of the airfoil. This may be accomplished via simultaneous processing of the opposite sides, or alternating side processing. Laser peening thin sections via either method can develop through-thickness residual compressive stresses. This creates a significant advantage, discussed in later sections, for retarding the crack initiation and its subsequent propagation. The through-thickness residual compressive stresses can be observed in Figure 14 for a 1.0 mm thick section of Ti-6Al-4V. The residual stress profiles for three processing conditions, low, intermediate and high are shown to a depth corresponding to the mid-thickness. The Ti alloys shown in Figures 12, 13 and 14, were laser peened using an opaque overlay.
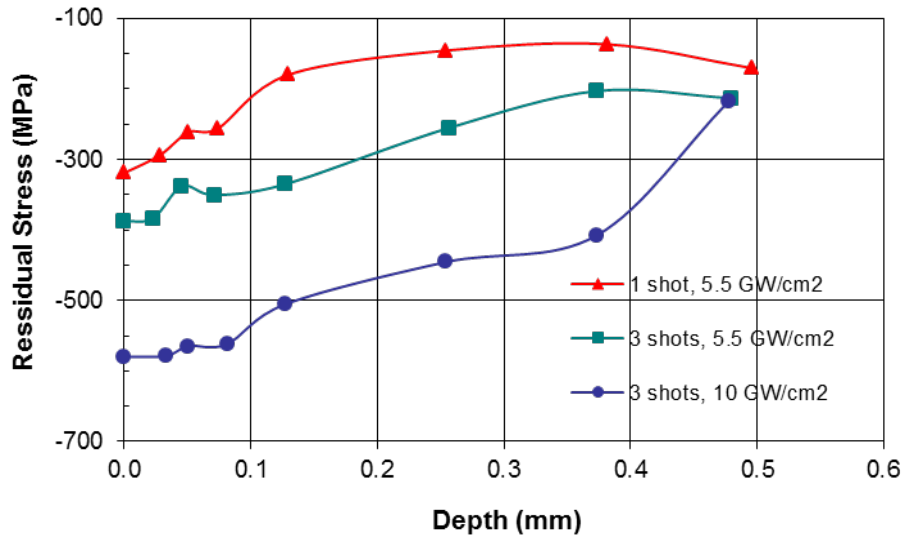

Figure 14. Residual stress profiles in 1-mm thick Ti-6Al-4V for three different laser peening conditions.

Another parameter that has effect on the depth of residual stresses generated is the spot size. The limitation in depth of the processing with small spots is a result of the two-dimensional attenuation of the shockwave. The shock front formed with small spots is smaller and therefore will decay below the HEL at shallower depths. Increasing the number of layers or overlap in a layer can compensate for the decrease in the depth of residual stresses. Figure 15 shows a comparison of the residual stress profiles produced by laser peening with different spot sizes and overlap in carbon steel [32]. The smaller spot size and lower overlap condition showed lower residual stress depth compared to the large spot size and higher overlap.
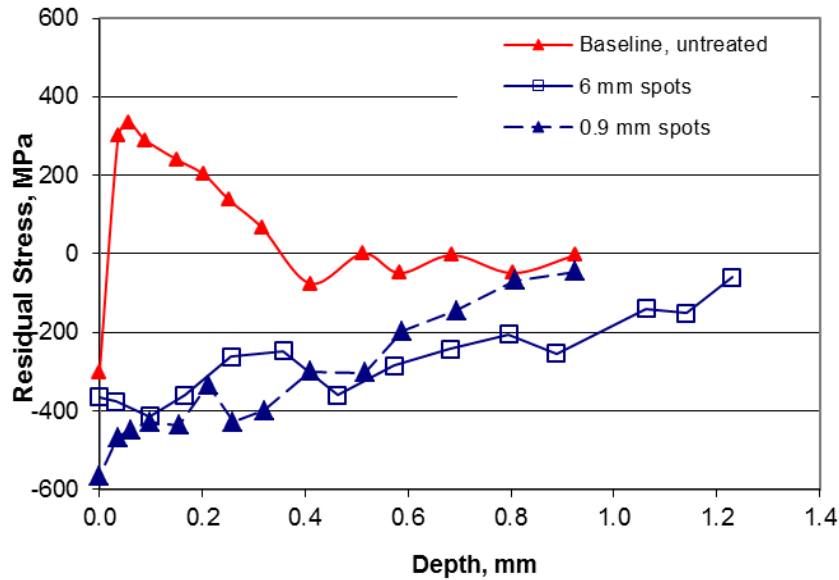
Figure 15. Residual stress profiles for 55C1 carbon steel, comparing large spots higher overlap and small spots lower overlap. The large spots had 50% overlap and the small spots had 25% overlap, 5 GW/cm². After [32].

Laser peening without an opaque overlay (Bare processing) will generate comparable high magnitude and high depth compressive stresses, although slightly lower than laser peening with opaque overlay. Processing without the opaque overlay still offers significant improvement over untreated and shot peened material. The residual stress originating from small spots for bare laser peening is shown in Figure 16 [19]. The smaller spot size and the shorter pulse length will yield lower depth residual stresses. This lower depth can be compensated for by applying higher number or layers, in this case higher number of impacts per area (36 impacts/spot). The residual stresses obtained are significant and extend 1 mm below the surface, much deeper than shot peening would be capable of producing. In this particular application the surface of the test coupons was purposely ground to generate a tensile surface stress in the untreated condition before laser peening.
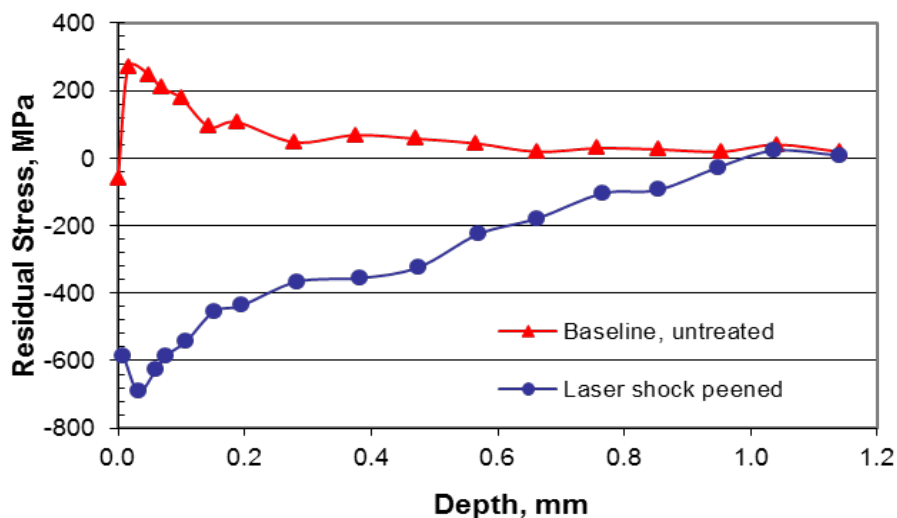

Figure 16. Residual stress profiles in 304 stainless steel after laser peening with 0.8-mm diameter spots, 36 impacts/spot, 5 GW/cm². After [19].

5.1.3 Residual Stress Stability in Laser Peened Alloys
Residual stresses generated by laser peening provide greater resistance to stress-induced and thermal-induced relaxation in comparison to conventional peening technologies. This benefit

allows laser peened components subjected to severe loading and temperature conditions to maintain significant beneficial effects of these residual stresses. This ability is attributable to two primary drivers. First, the lower amount of plastic strain (cold work) from laser peening reduces the driving force (activation energy) for dislocation rearrangement and annihilation at elevated temperatures. Secondly, the dislocation substructure introduced by laser peening relates to shock-induced substructures consisting of long dislocation tangles rather than the highly mechanically cold worked substructures produced by conventional peening.

For relatively intense laser peening conditions, plastic strains at the surface may range up to about 8% to 10% strain, but for most cases lies in the range from less than 1% up to 8%. This quickly drops to 1% below the surface. By comparison, shot peening introduces near-surface plastic strains as high as 20% to 40% or more [34]. Buchanan et al. [35] has presented a comparison of the thermal residual stress relaxation between laser peening and shot peening on IN100 exposed to 650 ºC for 100 hours. This study showed that shot peening lost around 50% of the residual stresses (maximum residual stress around -1600 MPa drops to around -750 MPa after thermal exposure). Laser peening only lost around 20% of the residual stresses where the maximum residual stress is near -1600 MPa drops to around -1250 MPa after thermal exposure.

Shepard et al. [36] performed thermal residual stress relaxation on laser peened Ti-6Al-2Sn-4Zr-2Mo at two exposure temperatures (370 ºC and 565 ºC) for two exposure durations (1 hr and 100 hrs). Figure 17 shows that the amount of relaxation of residual stresses is both temperature and exposure time dependent. At 370 ºC, the residual stresses become more-or-less stable after the first hour. The largest relaxation of residual stresses takes place near the surface where the largest plastic strain and the retained residual stresses are around 60% of the baseline values. As we go in-depth, the amount of relaxation drops and the retained residuals stresses at the largest depth are around 70% of the baseline. At 565 ºC, the residual stresses are almost fully relaxed. For Ti-6Al-2Sn-4Zr-2M, 565 ºC is top end of creep usage temperature and also near the range of temperatures used for annealing. So, it is expected that the residual stresses are not stable at this temperature [36].
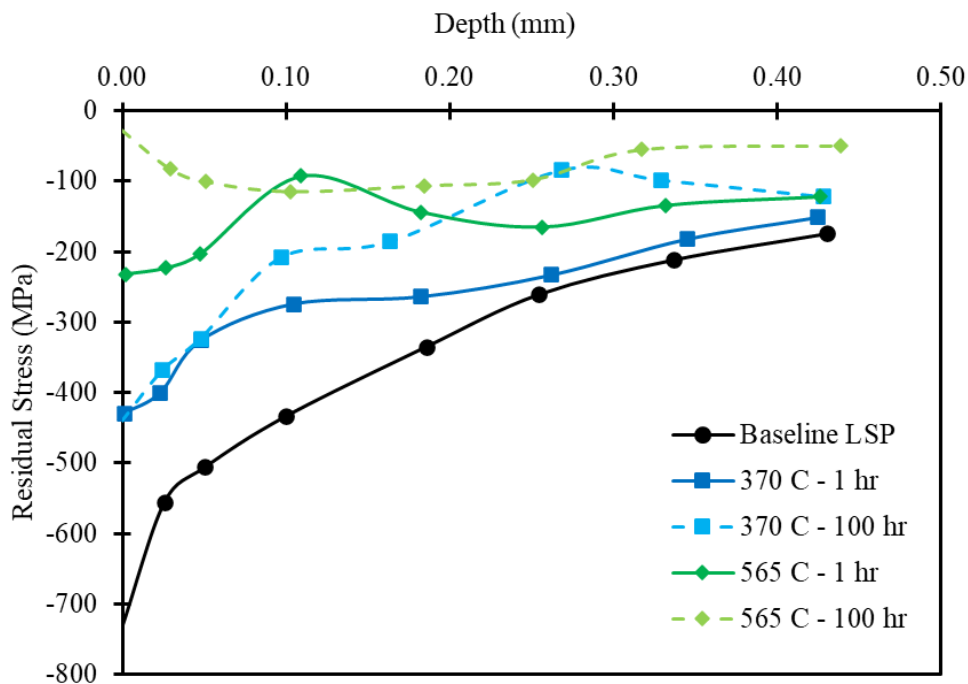

Figure 17: Residual stress versus depth profile of Ti-6Al-2Sn-4Zn-2Mo after exposed to 370 ºC and 565 ºC for 1 hr and 100 hrs. Per [36].

As can be seen in work of Shepard et al. [36] and several other researchers [37,38], there are three temperature regimes:

1) low temperatures where there is no residual stress relaxation.
2) very high temperature where there is full relaxation of the residual stresses.
3) intermediate temperature where a significant portion of the initial residual stresses is retained. In the intermediate regime, the majority of the residual stress relaxation occurs in the first few minutes up to an hour. After that, the retained residual stresses remain more-or-less the same for long exposure time.

5.2 Fatigue Performance Improvement by Laser Peening

The major driving force in the application of laser peening to a component is the increase in fatigue life and fatigue strength. The degree of improvement achievable with laser peening falls into two general categories. The most dramatic increases in fatigue performance are achievable in thin sections to prevent the propagation of through-thickness cracks into the structure from a stress riser associated with an edge, be it a hole, notch, corner, inclusion or other feature. Substantial increases in fatigue performance are also achieved in thicker structures laser peened on a single surface in the area of a stress riser or stress concentration. Examples of both of these categories are discussed in the following sections.

5.2.1 Fatigue Performance Improvement in Thin Sections

The earliest investigation of the effect of laser peening on the fatigue behavior of thin sections was performed on first stage airfoils in the F101 aircraft gas turbine engine [39]. In this investigation, the effects of shot peening and laser peening surface treatments on increasing the resistance of the airfoils to foreign object damage (FOD) were compared. A patch near the bottom of the leading edge of the blade was given one of three different surface treatments. One was a dual intensity shot peening representative of a typical process used on turbine airfoils; another was a high intensity shot peening intended to drive residual stresses deep into the surfaces; and the third was laser peening. The location for treatment was selected as being an area of high tensile stress in the airfoil, combined with having a high probability of being the location that FOD would occur. After treatment, the airfoils were notched to simulate FOD damage. Two types of notches were used, a 6 mm deep chisel notch having a plastic zone ahead of the crack tip, and a 3 mm deep electro-discharge machined (EDM) notch having a recast layer at the root of the notch. After notching, the airfoils were fatigue tested in a siren testing device to stimulate a specific vibratory mode.

The results of the fatigue testing are shown in Figure 18. The testing was conducted by starting at a stress amplitude of 20 ksi, running the test for 10^6 cycles, raising the stress amplitude to 30 ksi, running the test for another 10^6 cycles, and continuing this progression until the blade failed at less than 10^6 cycles at ah given stress load. Each bar in the graph (Figure 18) represents a test regime. The baseline, undamaged blade failed at 80 ksi. The notched, untreated blades failed at 20 to 30 ksi. The estimated average failure stress for the dual intensity shot peened blades was 35 ksi, and for the high intensity peened blades, 45 ksi. By comparison, the failure stress of the laser peened blades averaged about 100 ksi for the chisel notch, well above the failure stress of the undamaged blades, and at about the same level as the undamaged blades for the EDM notch. These results indicated that laser peening would enable a blade to continue to operate safely, although damaged by FOD at some level well above that previously viewed as cause for removal and repair of the blade. More recently, similar investigations on other turbine engine blades have shown comparable response to simulated FOD after laser peening [16].
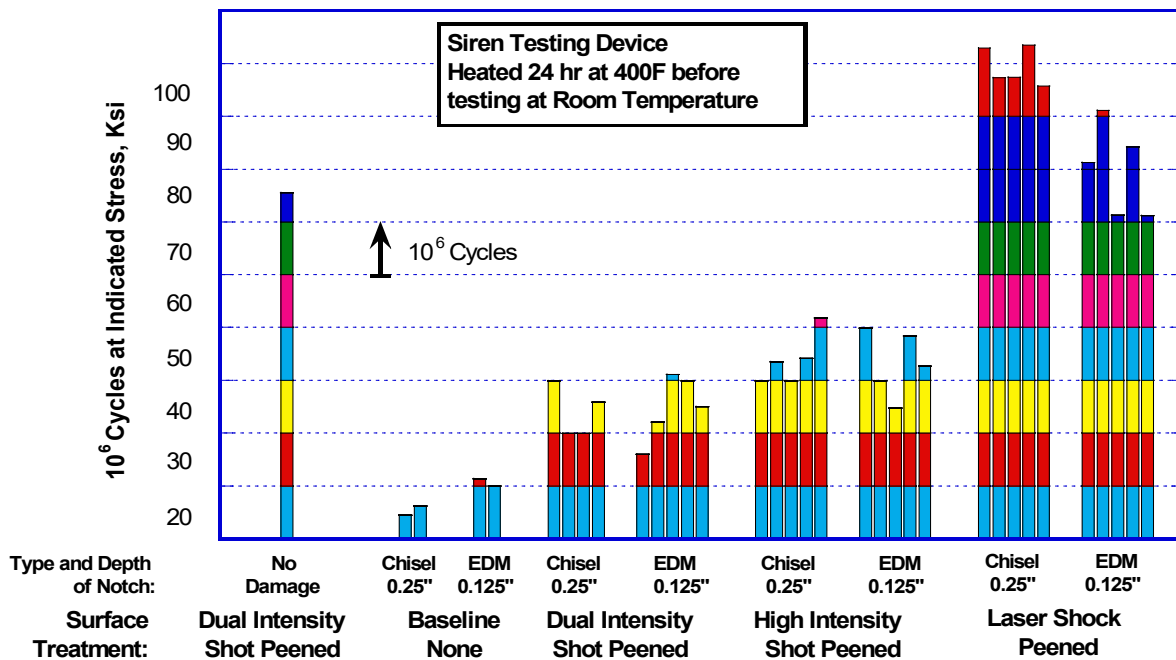
18

Figure 18. Fatigue of turbine engine fan blades showing a comparison of laser peening and shot peening for resistance to simulated FOD. After [39].

Investigation of the possible mechanisms for this dramatic improvement in resistance to FOD was performed on three-point bend specimens designed to simulate the leading edge of an airfoil [40]. A region in the center of the leading edge of the airfoil was laser peened, followed by notching in the center of the length of the laser peened region. The residual compressive stresses extended through the thickness of the blade after laser peening. The specimens were then fatigued in three-point bending to failure, while monitoring crack growth from the root of the notch. Figure 19 shows the dramatic effect of laser peening on crack growth rate. Without laser peening, the crack grew rapidly from the root of the notch, about 0.9 mm in from the leading edge. After laser peening, the crack grew slightly and then arrested. This behavior continued through a series of incremental load increases followed by incremental crack growth and arrest, until the crack finally propagated through the laser peened region or to failure.

Figure 20 shows the fatigue crack growth rate dependence on stress in terms of applied ΔK. The data shown is for R=0.1 where R is the ratio of the maximum to the minimum applied stress. The crack growth rates in the range of ΔK of 30-40 MPa m$^{1/2}$ are nearly three orders of magnitude slower than for the unprocessed material. At higher stress intensities, this difference lessens. This study also showed that at a higher R value, R=0.8, there was little difference between the unprocessed and laser peened crack growth rates.
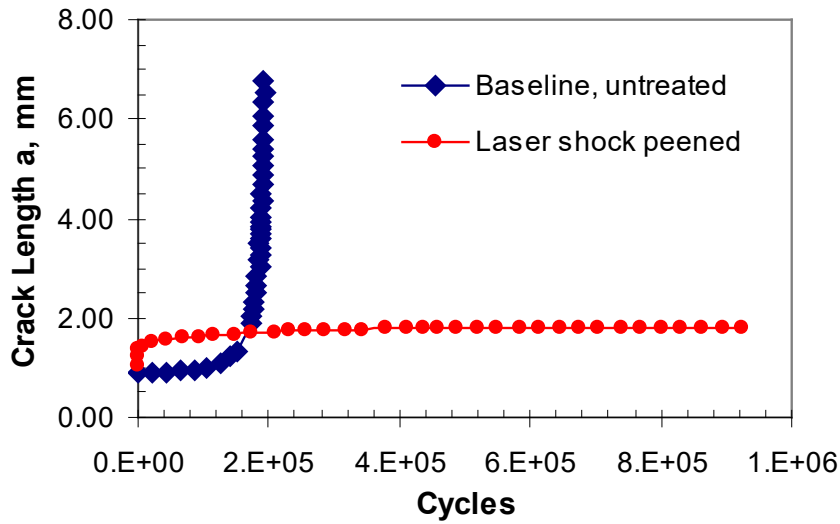
19

Figure 19. Comparison of untreated and laser peened crack growth rates for Ti-6Al-4V. Three-point bend, 9 GW/cm², 3 impacts/spot. After [40].
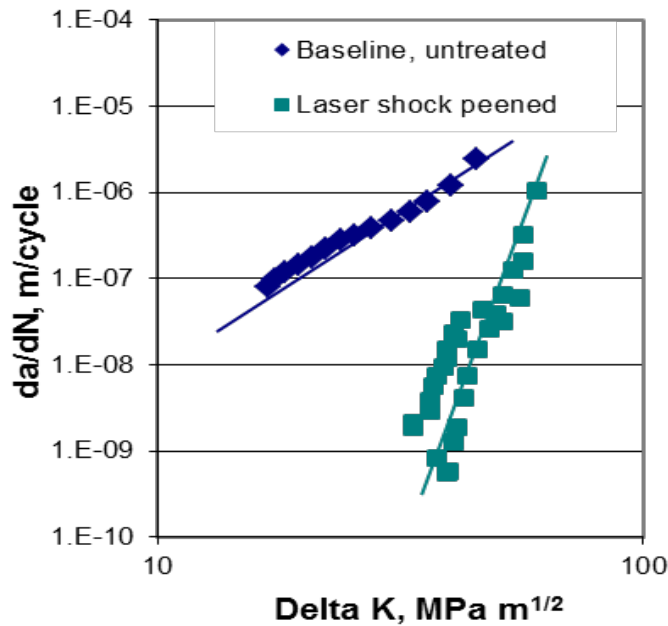

Figure 20. Fatigue crack growth rates for Ti-6Al-4V untreated and after laser peening. Three-point bend, 9 GW/cm², 3 impacts/spot. After [40].

The results indicate that the deep residual compressive stresses influence the crack growth rate by offsetting the applied stress intensities proportionally to the local compressive stress (superposition). When the stress intensities observed in testing the laser peened material were modified to account for the residual compressive stress, the resulting growth rates approach those observed in the unprocessed material. This effect has also been suggested for the effects of a crack propagating into a thick section from a laser peened surface [14].

5.2.2 Fatigue Performance Improvement in Thick Sections
In thicker sections, the fatigue-critical regions are typically features which act as stress risers, such as holes in shafts or lugs, fillets in parts such as crankshafts, and teeth or roots in gears. At these regions, the externally applied tensile forces that are amplified by the stress risers leads to crack initiation and propagation resulting in the failure of the component. In these cases, when the surface of the fatigue critical area is laser peened, the shock wave passes into the material and

20

develops a deep residual compressive stress below the surface. This residual compressive stress in the surface retards the crack initiation and subsequent propagation slowing the overall crack growth rate and extending component life. Once the crack has initiated at the surface, it continues to propagate into the laser peened surface within the compressive zone. The deeper the residual compressive stress, the deeper the crack must propagate into the component to reach the unpeened area, thus extending the component fatigue life. The combination of these effects can be used to increase fatigue strength and/or fatigue life.

One of the simplest test configurations to conduct for laser peening a fatigue critical region in a thick section is a 3- or 4-point bend test utilizing a large shallow notch. Only the notch surface is laser peened. As a result of the stress concentration from the notch, the crack must initiate and propagate into the material from the laser peened notched surface. There is evidence that laser peening significantly increases crack initiation time as shown in Figure 21 for 7075-T351 aluminum [22]. As can be seen in this figure, both laser peening and shot peening increased the number of cycles for crack initiation and crack propagation. Laser peening increased the life by ~7x compared to baseline whereas shot peening increased the life by ~2x compared to the baseline showing that laser peening has a 3x larger effect than what was observed for shot peening. The associated fatigue life curves are shown in Figure 22 [22,41]. Steels show a similar benefit as demonstrated in Figure 23 [32].
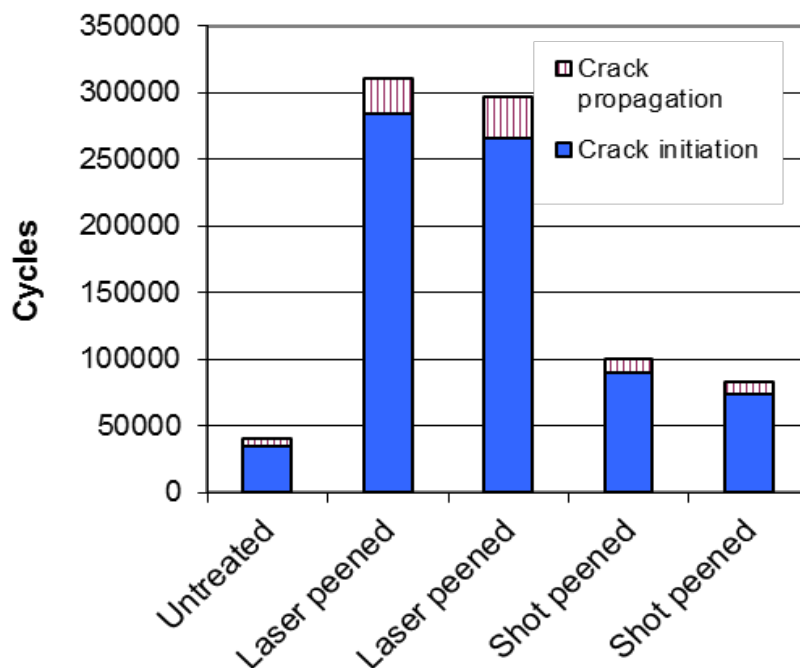

Figure 21. Comparison of the effects of shot peening and laser peening on crack initiation and propagation behavior in a 7075-T351 aluminum. Three-point bending, R=0.1, Kt=1.68, 4 GW/cm², 3 impacts/spot. After [22].
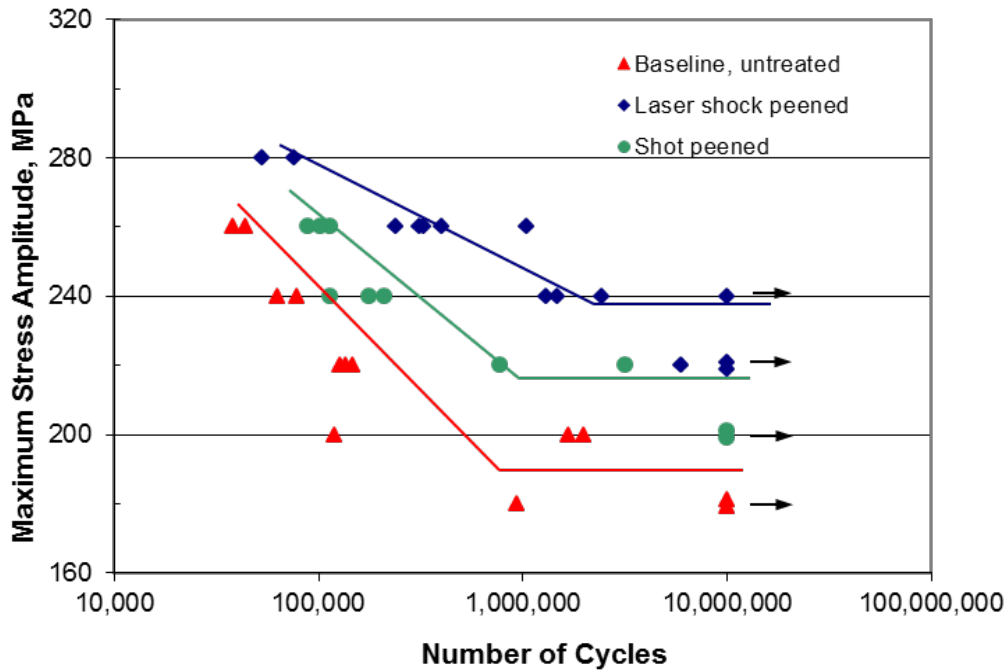
Figure 22. Comparison of laser peening and shot peening fatigue properties for a 7050-T351 aluminum in a typical stress life curve. 3-point bending, R=0.1, Kt=1.68, 4 GW/cm². After [22].
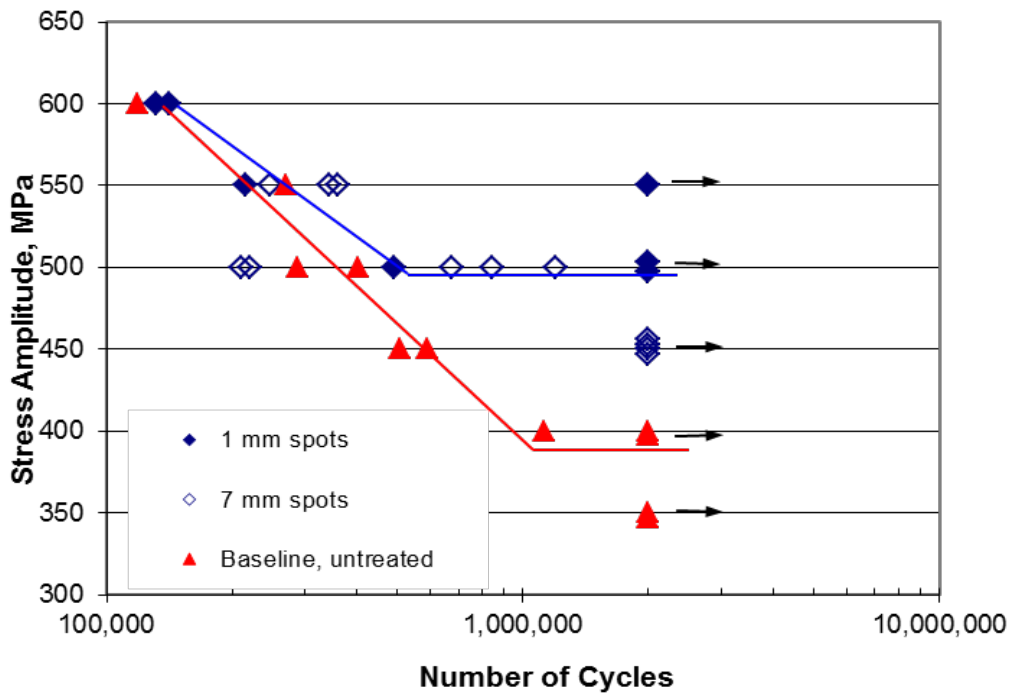

Figure 23. Effect of laser peening on the fatigue properties of 55C1 carbon steel, including the effects of large spots and small spots. Arrows indicate no failure at 2x10⁶ cycles. 4-point bending, 5 GW/cm². After [32].

5.3 Stress Corrosion Cracking Prevention

Stress corrosion cracking is a common failure mode in environments where corrosive environments are prevalent. Often these environments include marine atmospheres near the oceans or industries that use corrosive media in their processes. The development of stress corrosion cracking requires that three factors be applicable at the same time. These three factors are simply broken down into the following: tensile stress, corrosive environment, susceptible material. When all three of these elements are present, the material is susceptible to stress corrosion cracking and failure. A depiction of the stress corrosion critical parameters is shown in

Figure 24 below. Elimination of any one critical element will prevent stress corrosion cracking failures from occurring.
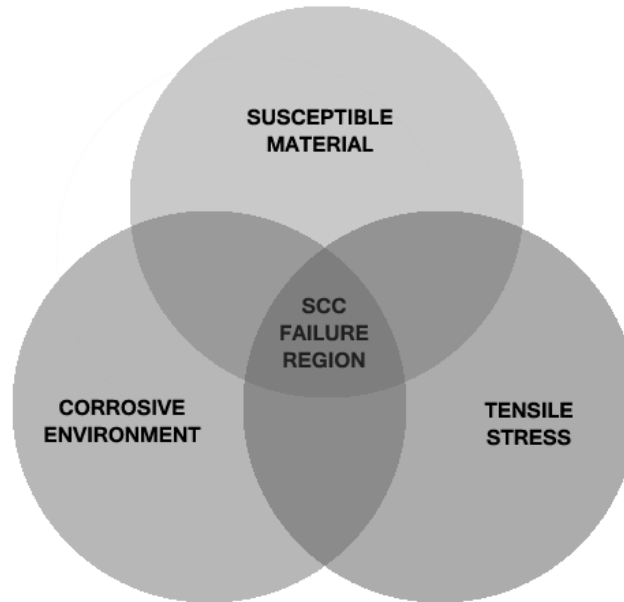

Figure 24. Critical elements required for stress corrosion cracking failures.

Laser peening has the benefit of combatting stress corrosion cracking. The deep residual compressive stresses generated by laser peening prevent tensile stresses at the surface (where the corrosive environment exists). Additionally, the increased corrosion resistance of laser peened materials reduces the corrosion potential of the alloys and prevents the corrosive effects of some media.

A testament to the prevention of stress corrosion cracking is 300M steel in the through hardened condition (typically greater than 1900 MPa tensile strength). At an applied stress of 75% yield strength (1240 MPa applied stress), stress corrosion cracking of this material in the as-machined condition produced failures at 250 hours. Shot peening provides some life improvement where the shot peened samples produced failures at 450 hours of exposure. Laser peened samples exposed to the same conditions produced no failures after 1500 hours [42].

5.4 Environmental & Pitting Corrosion Resistance
Laser peening parts not only decrease the sensitivity of materials to the detrimental effects of corrosion, it can also aid in preventing corrosion. In 2024-T351 aluminum, potentiodynamic tests showed anodic current density shifts after laser peening, indicating pitting resistance for both initiation and propagation [43]. There was also a reduction of the passive current density on laser peened surfaces, indicating increased corrosion resistance. Carbon steel has also shown a change in corrosion resistance after laser peening [14]. After exposing a carbon steel plate, having a small laser peened area, to an aqueous environment, the entire plate was corroded except for the laser peened area on the surface. In this case, it was suspected the surrounding unpeened material acted as a sacrificial electrode with respect to the higher equilibrium potential of the laser peened material.

Improvement in corrosion and pitting resistance were also observed in laser peened stainless steels. Corrosion potentials and pitting behavior were investigated in a martensitic, 12% Cr stainless steel, Z12CNDV12-020, used in steam turbines, and for an austenitic stainless steel, 316L [29,30]. The laser peened areas ranged from 1 cm^2 to 4 cm^2. The 12% Cr steel was exposed to a 0.1M NaCl + 0.01M Na$_2$SO$_4$ solution [44]. Increases in the free potential of between 30 and 100 mV were found, indicating increased corrosion resistance. The effectiveness of laser peening increased with a shorter pulse length and higher power density. Potentiodynamic measurements

showed that laser peening reduced the passive current density from 1.2 $\mu A/cm^2$ down to 0.5 $\mu A/cm^2$ in the 12 % Cr stainless steel. The pitting potential was nearly constant before and after laser peening, but laser peening prevented pit initiation on inclusions in the material surface.

Pitting behavior of untreated, laser peened and shot peened surfaces in 316L stainless steel was also investigated using a statistical approach [45]. In this approach, groups of specimens are simultaneously exposed, and a non-survival pitting probability is determined at increasing potential values. The results for untreated and laser peened surfaces are shown in Figure 25. It is clear that the surface treatment results in a significant anodic shift in the pitting potentials for the laser peened surfaces. Laser peening produced significant pitting potential shifts, up to +100 mV. After shot peening, not shown here, the effect is intermediate between the untreated and laser peened results, producing a shift at lower potentials only, below 420 mV. The degree of improvement possible with shot peening was possibly limited by the presence of the martensite and the higher surface roughness. In addition to the shifts in pitting potential, the slopes of the curves are increased by both treatments, possibly indicating a change in pit initiation mechanism.

These beneficial effects of laser peening have been tentatively attributed to the compressive surface stresses reducing the detrimental effect of surface inclusions as pitting initiation sites, and to possible modification of the growth kinetics of passive layers [45].
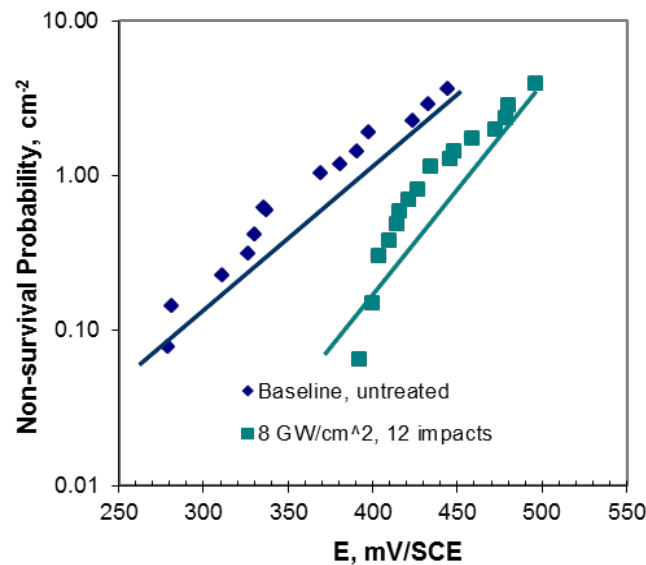

Figure 25. Statistical probability treatment of pitting corrosion of 316L stainless steel, laser peened and untreated. After [45].

6. Laser Peening Development Program Structure
Industrial laser peening development programs benefit from all the previously presented information to provide the optimized production services or equipment sales to meet customers' requirements. Figure 26 provides an example of a typical laser peening development program structure. The first step of the process is design analysis, at this step all the information around the customer component such as part geometry, loads, failure locations, etc. are analyzed. The second step in the process is laser peening engineering design. At this step, the design of the laser peening conditions and locations takes place, and it utilizes database information of the response of different material and different geometries to various laser peening conditions coupled with simulations that enables prediction of the resulting residual stress and component life enhancement on the customer component. The third step is application verification and validation. This step can have few subtasks that takes place in series or in parallel depending on the customer's approach. These subtasks include performing laser peening on representative components and various residual stress and tests are performed; performing laser peening on the

actual customer component; and assessing the in-service benefits from laser peening. Once the benefits of laser peening have been demonstrated on in-service components, the laser peening process parameters are locked and production as a service or equipment installed at the customer facility launches and ramps up. The final step is the production life cycle sustainment. In this step there are different quality control procedures that ensure the quality of the laser peening process and desired performance of the components. Some of the quality control procedures include live monitoring and full data collection of the laser peening parameters and process parameters, routine components inspection and testing.
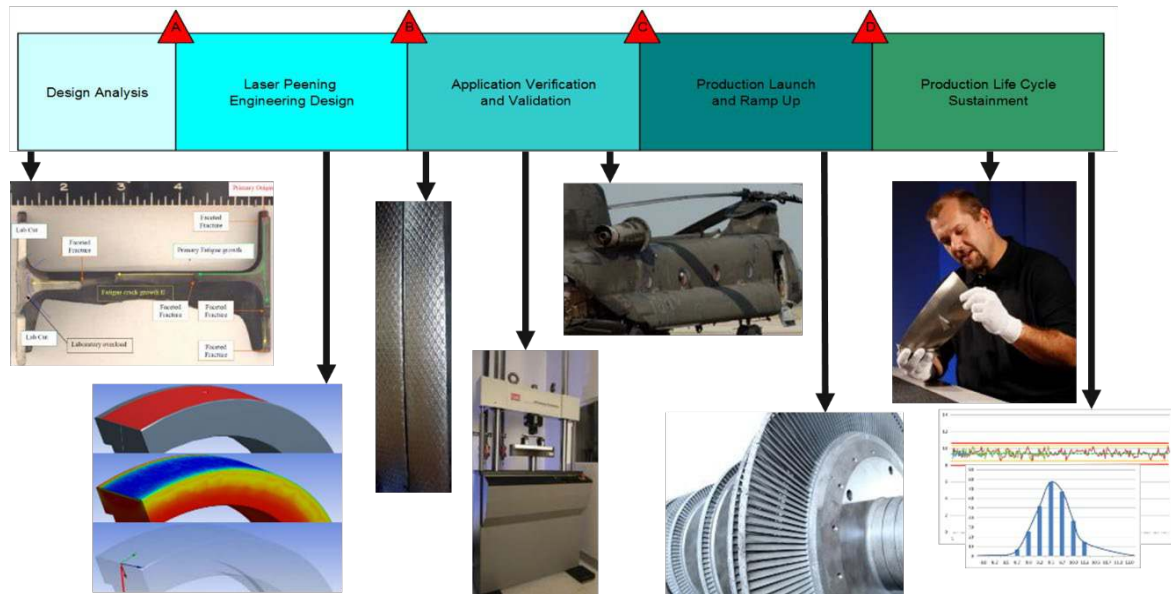

Figure 26: Laser Peening Development Program Structure

7. Laser Peening Modeling and Simulation

Industrial and academic efforts have progressed the modeling and simulations capabilities related to laser peening. Modeling is concentrated into two separate but equally important areas. The first area deals with the shockwave formation, propagation and material interaction [10,46,47]. This area has been mainly investigated by academics in efforts to understand the physical and microstructural changes resulting from laser peening. The second aspect of the modeling revolves around the in-material effects, such as the residual stress distribution [48,49]. This area has been greatly beneficial for industry where advancements in analytical modeling of residual stresses have significantly reduced the implementation time of laser peening. The ability to predict the benefits of the process analytically has reduced design and optimization time and enables processed parts to enter service on a shortened timeline. Empirical and finite element models have been developed for both fields of study. Simulations of the direct process required using finite element software with dynamic analyses capabilities; however, the process effects can be modeled using static finite element analysis software.

7.1 Shockwave Formation, Propagation and Material Interaction
7.1.1 Shockwave Formation Modeling

Significant effort has been devoted to modeling the laser beam interaction with the surface of the material being laser peened in order to predict the peak pressure of the shock wave. An early approach used the "Piston Model" to predict the peak pressure and the pressure temporal profile for confined plasma. In this approach, the energy of the laser beam interacting with the plasma is partitioned into two parts, one of which is absorbed by the plasma and increases its temperature and thereby its pressure, and the other which ionizes the plasma. The energy partitioning parameter is determined by calibrating the model with experimental results. This model predicts $P_p \propto I^{1/2}$, in agreement with experimental data, where P_p is the peak pressure, and I is the peak irradiance of the laser beam. The energy absorbing partitioning parameter varies over a range of

0.2 to 0.5, and at present must be experimentally determined for specific overlay and other processing conditions [46]. A recent publication by Pozdnyakov and Oberrath [50] modeled the plasma created by laser peening and the resulting peak pressure of the shockwave propagation into the material.

7.1.2 Shockwave Propagation and Material Interaction
The shockwave propagation and its interaction with the material has been simulated using molecular dynamics simulations and mesoscale simulations using dislocation dynamics.

7.1.2.1 Molecular Dynamics
Molecular Dynamics (MD) can provide great insight about the material response to shockwave propagation at molecular scale where in-situ measurement and characterization of material dynamics at ultra-high strain rates is not currently possible. Two major examples are phase transformations and interfacial strength of defect microstructural features. However, due to limitation of simulation volume and time, MD simulation usually covers strain rates of 10^8 and above, pulse durations in picoseconds (ps) and very small crystal volume which has its differences compared to the ns pulse duration laser peen of polycrystalline material that has been described up to now in this chapter but could be very important for the new emerging femtosecond (fs) laser peening processes described in the last section of the chapter.

Meng et al. [51] simulated Al-Cu alloy subjected to LSP pressures at various temperatures to study the microstructural alterations as the shockwave transmits the crystal lattice. The work covers pulse duration of 10 ps and shows strain rate transformation processes and dislocation formation at different temperatures. Li et al. [52] showed that laser shock wave can create delamination of microstructures. Duport and German [53] presented the change in the microstructure at different strain rate shock loading for single crystal copper.

7.1.2.2 Mesoscale Simulations Using Dislocation Dynamics (DD)
Several groups around the world utilize simulation codes that combines discrete DD analysis with continuum finite element analyses. These models have been utilized to investigate various microstructural analysis including shockwave material interactions. Wang et al. [54] investigated the change in the stress-strain curves, dislocation densities and deformed microstructure at different strain rates between 10^4 to 10^6 for fcc single crystal. The microstructure at 10^6, strain rate of typical ns laser peening process, showed the high activity slip bands with dislocation entanglement. Kattoura [55] showed that for copper single crystals, the microstructure remains slip bands and dislocation entanglement with heterogeneous dislocation nucleation (activation of Frank-Read dislocation sources) up to strain rate around 10^7. Afterward, homogeneous dislocation mechanism becomes the dominant mechanism which leads to avalanche of dislocation microstructure. Even though these investigations were on single crystals, these findings are in agreement with several experimental studies that investigated the microstructure after laser peening on various polycrystalline materials [56,57].
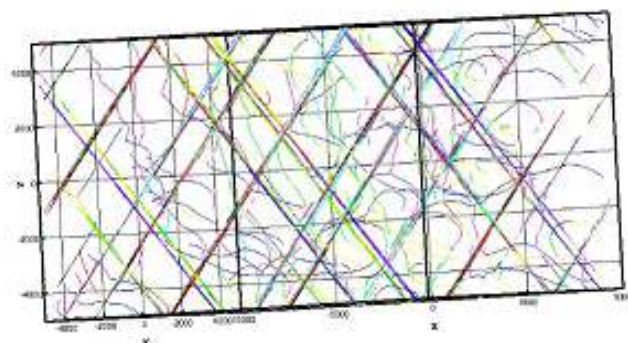

Figure 27: DD simulation showing slip band activity and dislocation entanglement for shock loading at strain rate 10^6. Per [55].

7.2 Residual Stress Modeling

The residual stress profiles developed by laser peening are of particular interest because they directly affect the way the material responds to stress- or environment-related service conditions. Results are dependent on the composition, microstructure and geometry of the part being evaluated, its surface condition and topology, and the pressure profile applied to the surface by the laser peening conditions used. Addressing all of these considerations when evaluating or optimizing the laser peening conditions for a new or modified application often adds time and cost to the evaluation unless there is closely allied experience available from a previous, similar application. Therefore, simulating the developed residual stress profile and distribution in a component enables optimization of processing for increased resistance to failure from fatigue, stress corrosion cracking, fretting fatigue, and wear.

Modeling of the residual stresses in a material can be accomplished via several different methods. The different models and techniques incorporate different aspects of the process for studying the in-material effects and vary in terms of software requirements and required capabilities.

7.2.1 Dynamic Modeling of Shockwave Effects for Residual Stress Development

Several methods of modeling use the pressure pulse induced by the shockwave as a dynamic load in finite element models. The material effects can then be evaluated via elastic-plastic simulations, or via strain hardening effects. Unfortunately, at present, there exists little to no actual material property data available in the strain-rate range required for this type of modeling (10^4 sec^{-1} to $>10^6$ sec^{-1}). As a result, the approach generally adopted for dynamic modeling has been to modify the material properties in the software library to correlate the model predictions with known experimental data. The expectation from this approach is that the calibrated material properties will be consistent over a given range of input variables. A result of this modeling approach for Ti-6Al-4V is shown in Figure 28 for two peak pressures. The model was first calibrated to fit the residual stress profile measured for 5.5 GPa peak pressure. Then, the stress profile for a peak pressure of 8.3 GPa was calculated independently by changing only the pressure profile. The fit of the predicted residual stress for 8.3 GPa peak pressure to the actual measured results was excellent. However, this approach does require that the model must be independently modified for each alloy, and possibly for different heat treatments that change the alloy properties significantly.
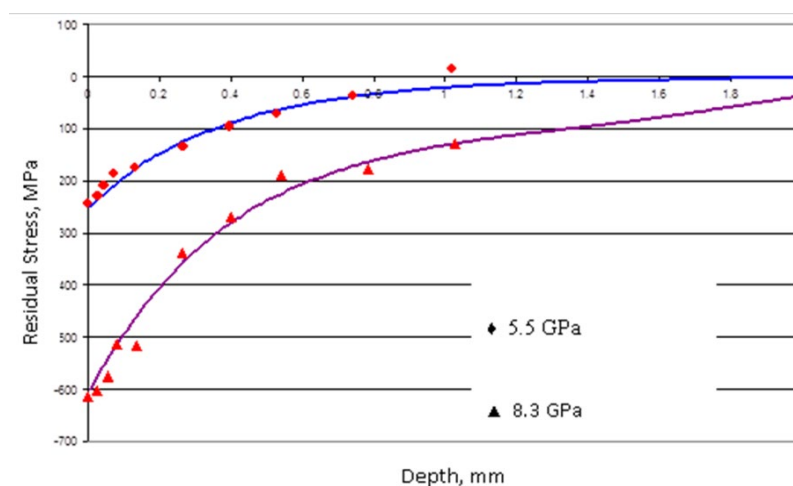

Figure 28. Comparison of experimental and modeled residual stress profiles for two peak pressures.

The work by Kim [58] highlights many model parameters that are optimized in explicit analyses including the mesh size, stability time limit, and solution time. The work also provides insight into residual stress optimization based upon peak pressure, duration, spot size, and multiple impacts. Frija [59] work provided a similar approach with a higher emphasis on total optimization of a residual stress profile in terms of the shape. In both articles, the authors utilize the plasma

pressure equation proposed by Fabbro almost three decades ago. Similarities also exist in the usage of the Johnson-Cook strength model as being the primary used. Amarchinta [60] provides an overview of the accuracy of various material models fit to experimental data and provides a reasoning behind Johnson-Cook model being the most commonly used. Sun [61] provided a comprehensive study on the effect of various laser peening parameters such as power density, number of shots, spot size and laser pulse duration of the residual stresses. Li [62] conducted an experimental and simulation study of the residual stresses generated by laser peening of titanium. The work investigated the effect of the beam energy distribution (flat-top vs gaussian) and the effect of various energy levels for each beam on the resulting residual stresses.

7.2.2 Eigenstrain Modeling of Shockwave Effects for Residual Stress Development

An alternative method of modeling that has gained wide acceptance and usage is referred to as the eigenstrain method [63]. The eigenstrain method of modeling is based upon the elastic response of a material to inelastic strains (termed eigenstrains [64]). This method of modeling is capable of predicting residual stresses from plastic deformation, thermal expansion, phase transformations, and other non-bulk effects. It is particularly useful for surface modification procedures, such as laser peening, and can be performed with static finite element analysis. The eigenstrain method also has the benefit of being geometry independent. Once a model has been developed for a particular type and thickness of a material, it can be applied to other geometries. The usual practice is to develop the model from simple geometries and thereafter use it in modelling more complex geometries.

The model development requires input from one of two different areas. Typically, the residual stresses in a simple geometry that has been laser peened are first measured and the corresponding strains that generated the residual stress are calibrated in a finite element model. An alternative to this method of eigenstrain calibration is to use calculated strains from an explicit FE model. After calibration, application of the laser peening in the model geometry of interest is carried out via a thermal expansion simulation with a 1 degree temperature increase to generate equivalent eigenstrains.

Details on eigenstrain modeling, calibration, and applications are readily available in the literature [63,65,66]. It is probably the most commonly employed modeling technique for evaluating the residual stresses that will develop in a component from laser peening. The static analysis offered by the method is much less computationally expensive than dynamic methods and typically yields very accurate predictions. An example of an eigenstrain based residual stress model of a laser peened surface is shown in Figure 29. This specific model was developed at LSP Technologies. The results are an extension of a calibrated eigenstrain model derived from a rectangular block that was subsequently applied to a curved surface. This particular application is based on a high strength steel (>1650MPa yield strength).
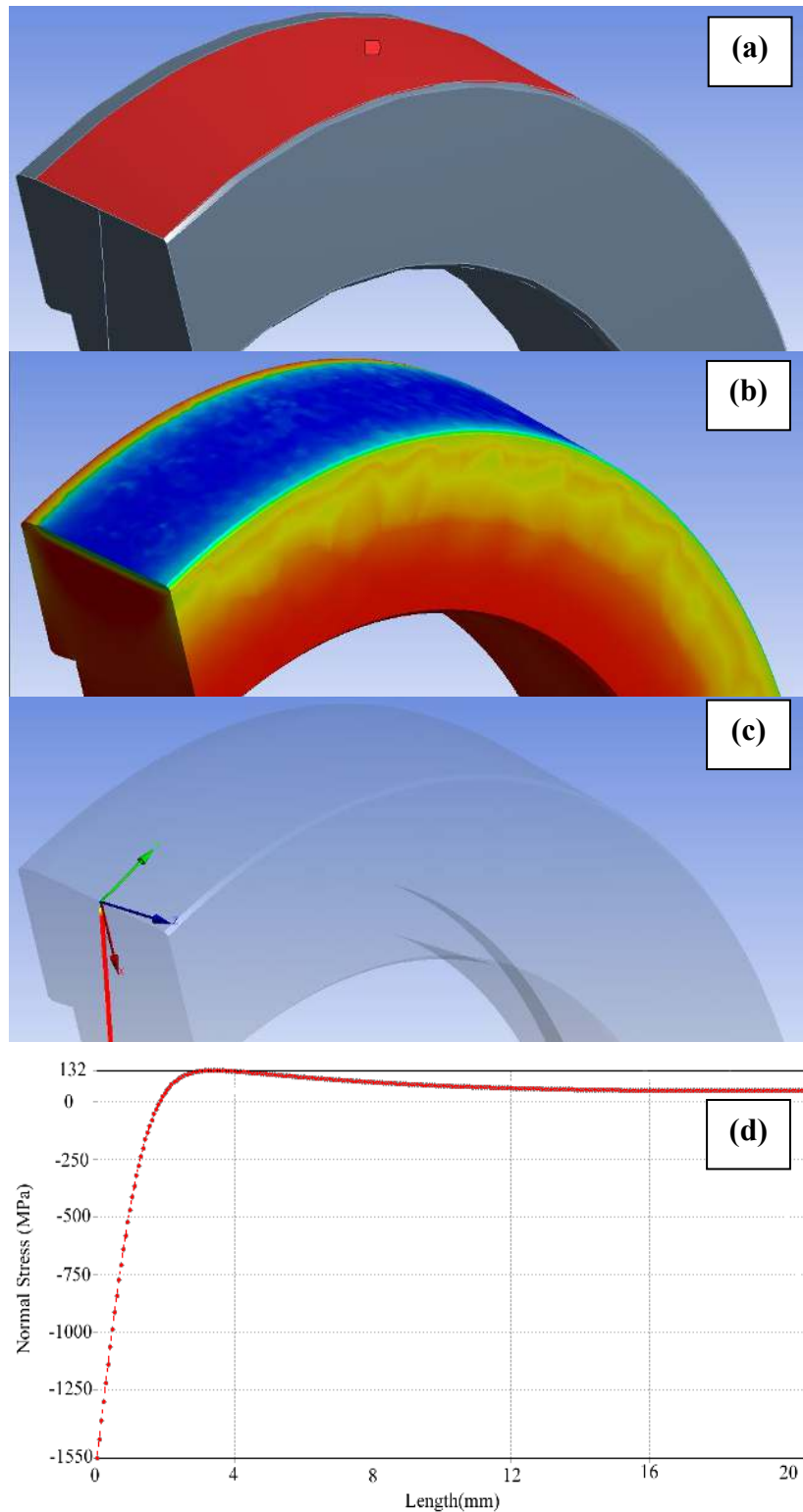
Figure 29. Eigenstrain modeling of residual stress distribution from laser peening: a) depicts surface to be laser peened, (b) depicts residual stress distribution across surface and through cross section, (c) displays the residual stress distribution along a surface-normal line through the cross section with charted results shown in (d).

Eigenstrain modeling for residual stress prediction and thus laser peening process parameters optimization has matured in the last few years and became a critical step in the applications development programs as discussed in section 6. Eigenstrain modeling has provided the ability to predict the residual stresses in complicated geometry components and in thin geometries which have previously been challenging applications [67]. Figure 30 provides examples of the results of eigenstrain simulation performed at LSP Technologies on (a) complicated geometry component and (b) thin geometry blade edge.
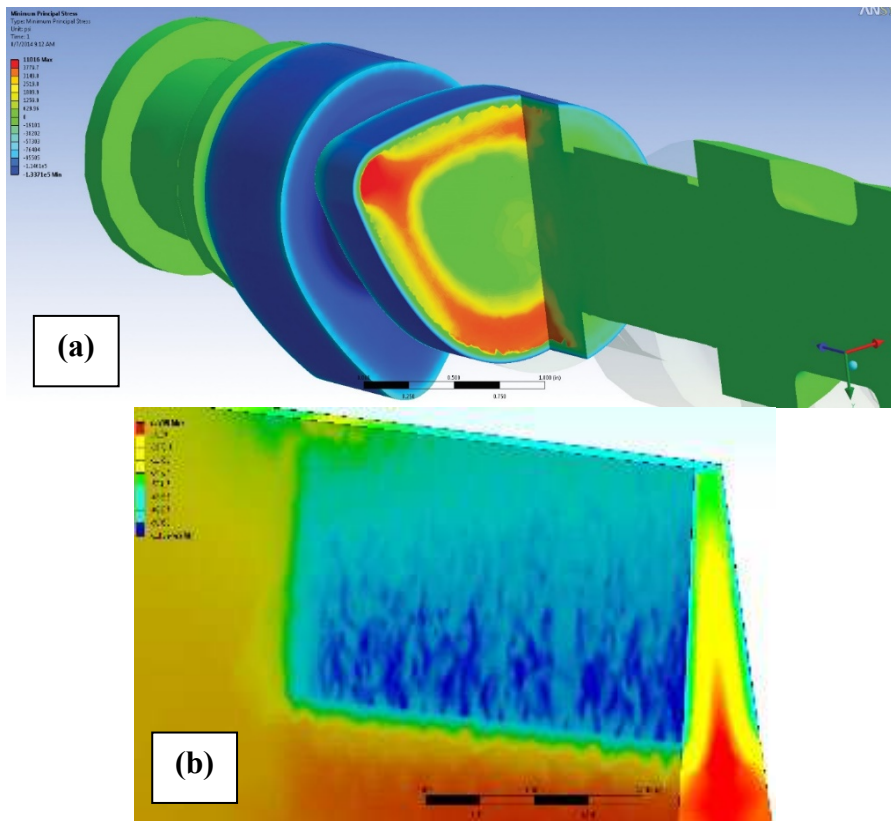
29

Figure 30: Eigenstrain simulations on a) complicated geometry component and b) thin geometry blade edge.

7.3 Plasticity Modeling with Complex Shockwave Interactions

Modeling of laser peening thin sections from both sides simultaneously requires even higher levels of sophistication. In the case of double-sided laser peening, the shock wave interactions within the material are much more complex and numerous than they are in single-sided processing. Not only do the shock waves entering the material from opposite sides interact with each other on their initial traverse through the thin section, but they become tensile reflected waves, and both the tension and compressive waves produce numerous release waves from their periphery as they reflect from the opposite surfaces. Figure 31 shows the complexity and large number of stress wave patterns and interactions occurring in a 1-mm thick section. As the section thickness decreases, the initial interactions of the shock waves become stronger because there is less attenuation of the waves before they begin to interact. Also, the number of interactions becomes more numerous, because the number of reflections from the opposite surface within a unit of time increases. Each time these stress waves interact as compressive or tensile waves in various combinations, if their combined peak stress is above the dynamic yield strength of the material, local plasticity will occur. Thus, at various locations within the material, reversed plastic deformation may occur numerous times before the stress waves attenuate to the point where no more plastic strain occurs.
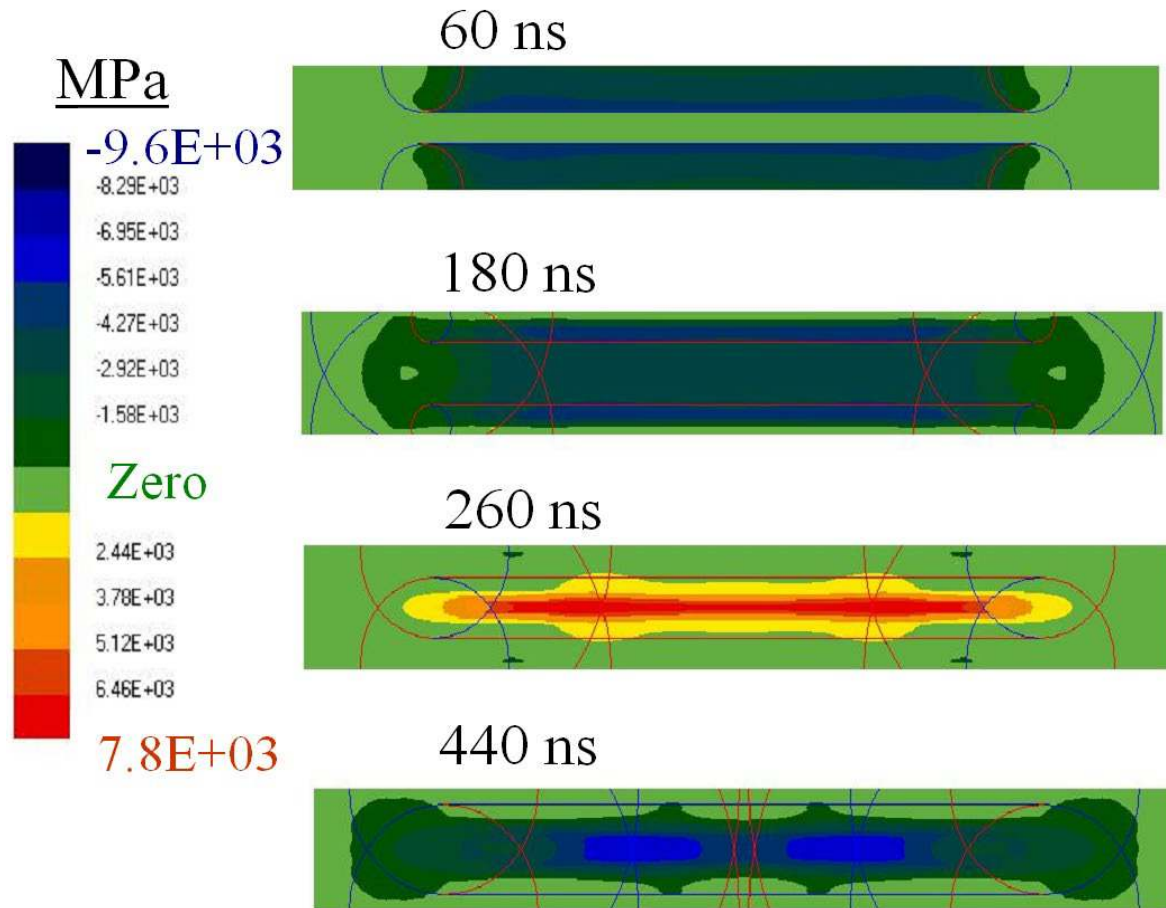
Figure 31. Modeled stress wave interactions in a 1-mm thick section laser peened from opposing sides. The darker lines are compressive stress waves, and the lighter lines are tensile stress waves.

8. The Future for Laser Peening

The future of laser peening is one of continuing advancement in production applications, technology development and scientific research. The technology is being seriously pursued on these fronts across the globe and particularly in the U.S.A., France, Japan, China, Spain, Australia, Germany, England, Czech Republic, South Africa, Singapore, Mexico, and India. Previously, the biggest barrier to wider application in manufacturing has been the relatively high cost, and to a lesser extent, the slow throughput of the process. While once limited to high dollar, high risk parts, such as aircraft engine compressor blades, the advent of new processing technologies has enabled many new markets. Applications in aerospace, industrial tooling, medical implant devices, automotive and commercial trucking, marine industry, performance racing, and several others are currently entering commercial production. With select companies offering the sale and lease of laser peening equipment, many organizations are bringing the technology in-house. This further expands knowledge about the process and enables application of the technology to new ideas.

A few advancements in laser peening applications are worth mentioning in this section since they have great potential in the near future.

8.1 3D LSP – Hybrid Additive Manufacturing Process

The application of laser peening on finished additive manufactured (AM) parts has shown great benefits to various material properties especially fatigue life [68]. However, Kalentics and coworkers [69] have been investigating a hybrid approach that incorporates laser peening in the AM process. This process is currently manual, in which the sample is removed out of the AM machine after a set number of layers, laser peening is applied, then the sample is placed back in the AM machine for the continuation of the build. This approach is providing higher depth of

compressive stresses, lower porosity, healing cracks and further improvement in fatigue performance. These findings provide an opportunity for industrial systems that integrate the laser peening process as part of the AM process in a fully automated system.

8.2 Laser Peen Forming and Laser Peen Straightening

With the emerging needs for higher precision forming technologies, the laser peening process, which is known for its high levels of controllability and repeatability, is being utilized for forming components in a process known as laser peen forming. Laser peen forming is benefiting from the advances in the simulation and prediction of not only the residual stresses but also the plastic deformations and thus predictions of full component deformations. Figure 32 shows both the simulation of the laser peen forming process on 6 ft x 4 ft x 0.375" thick aluminum sheet and the corresponding resulting laser peen formed sheet processed at LSP Technologies [70]. Yocom et al. [71] provided a review paper that summarizes the research and development status of laser peen forming.
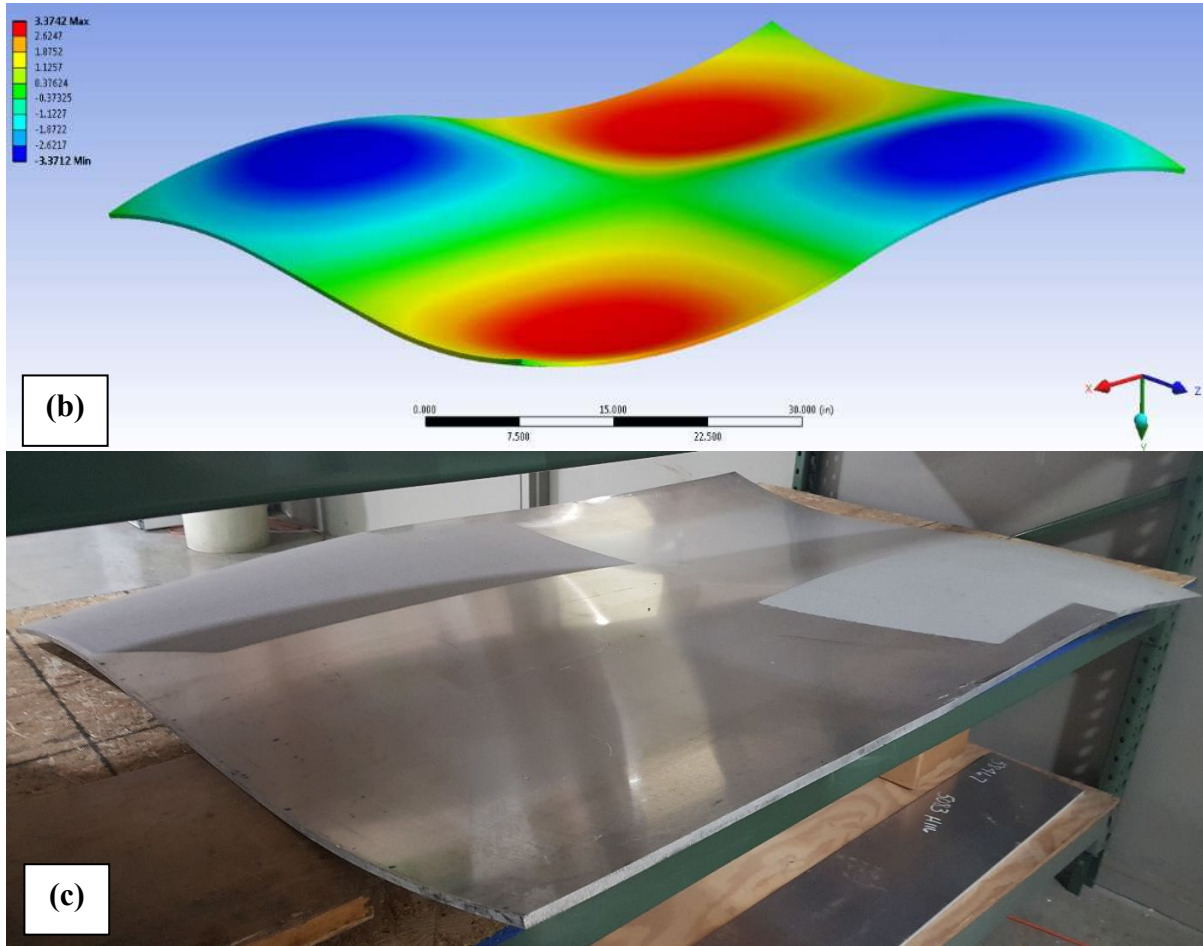

(a)
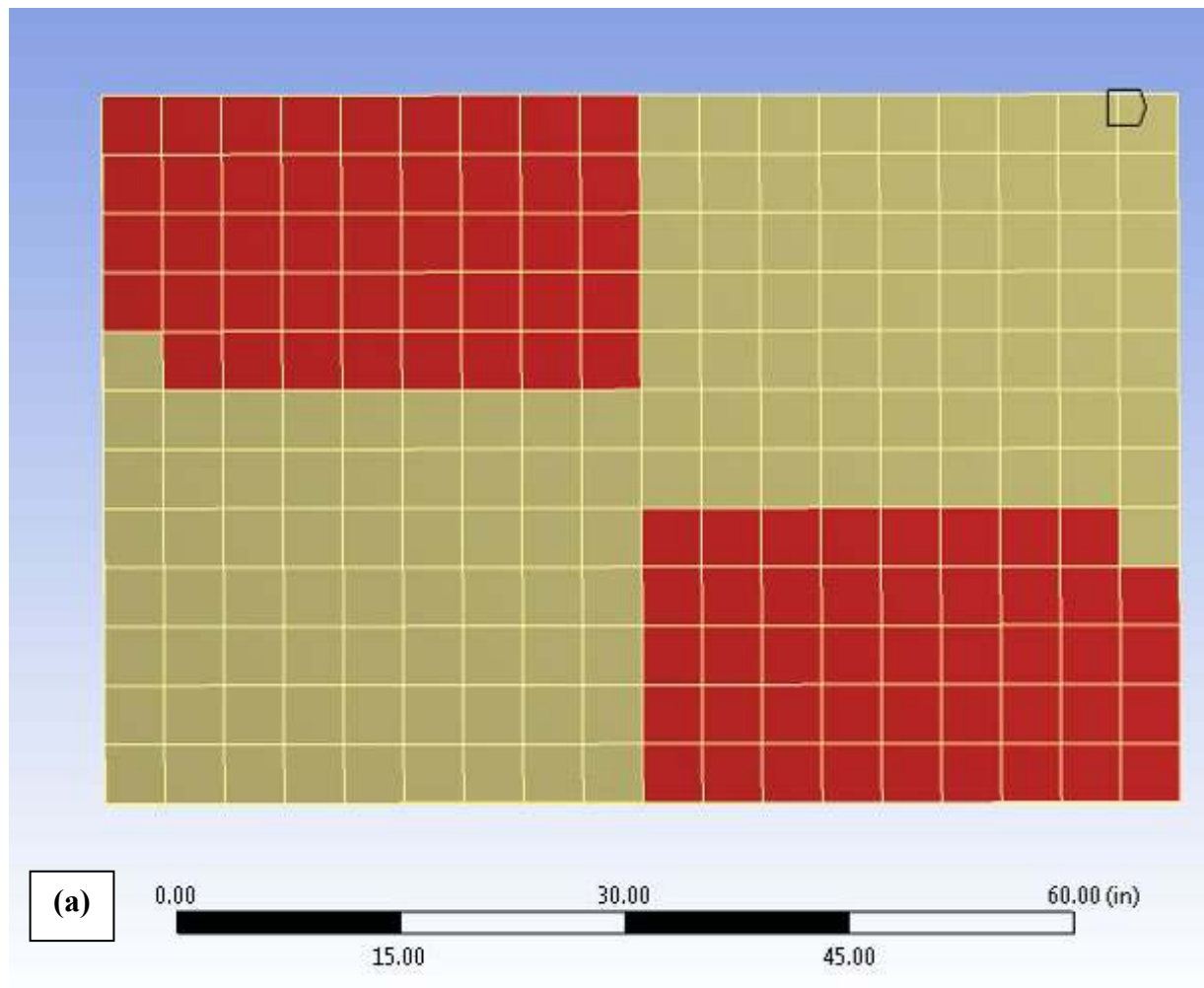
Figure 32: Laser peen forming of 6 ft x 4 ft x 0.375" thick aluminum sheet by LSP Technologies a) laser peening pattern, b) simulation of the formed shape and c) actual laser peen formed sheet.

On the other hand, the same concept is being utilized for laser peen straightening out-of-tolerance components. This field has been gaining attention due to its ability to reduce scrapped parts. Contrary to other currently used correction methods, laser peening has the precision and adaptability to build a closed-loop feedback system that can correct out-of-tolerances of variable magnitude and different direction curvature. Figure 33 presents an example of laser peening straightening on Wankel crankshaft. Laser peen forming was able to provide straightening within 0.004 mm which was consistently within the 0.010 mm maximum specification of the customer.
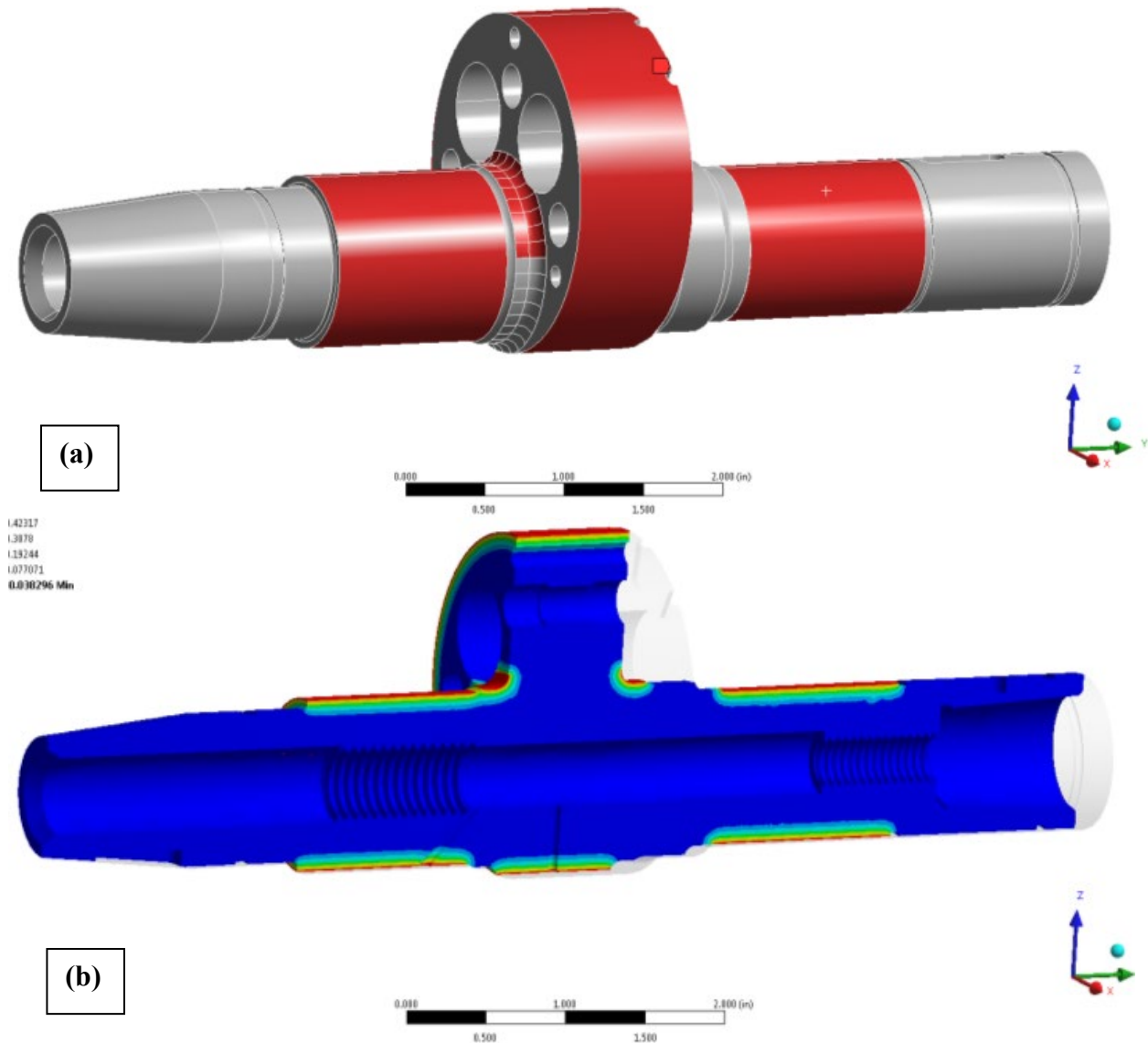
Figure 33: Laser Peen Straightening of Wankel Crankshaft: (a) laser peening pattern; (b) simulation of the laser peened form.

8.3 Shot Peening Replacement

Historically, laser peening has been offered as a replacement for shot peening for applications that require deeper residual stresses. Recently, and with the advancement to the size and cost of laser peening equipment, laser peening is being pursued as replacement for shot peening for processing control and cleanliness factors while maintaining the same residual stress requirements as legacy shot peening processing. Laser peening provides much higher levels of controllability and repeatability as a process, eliminating inconsistencies of the shot peening process and eliminating the need for tedious part masking processes. In addition, laser peening using laser beam instead of shot media, eliminates problems of media penetrating to component location and becoming the causes of failures. Finally, laser peening equipment has much smaller footprint and offer clean working environments compared to shot peening areas that has media scatter around in addition to dust from the process.

8.4 Femtosecond Laser Peening

A new emerging research and development area is femtosecond laser peening. The traditional laser peening systems discussed in this chapter utilize lasers with pulse durations in the nanosecond regime. Femtosecond laser applications are expanding to different industries. Biomedical applications such as eye surgery Laser Assisted In Situ Keratomileusis (LASIK) are the most commonly known applications [72]. In addition, femtosecond lasers are utilized in

various manufacturing applications such as surface texturing, micromachining, thermal writing of photonic devices in glass and polymers and others [73]. Sano et al. [74] demonstrated laser peening using femtosecond lasers without the need for any overlay on 2024 aluminum alloy. The laser peening process took place without the use of either opaque or transparent overlays which they referred to as under atmospheric condition or "Dry Laser Peening". This process was able to induce compressive stresses of magnitude -300 MPa and depth of around 0.1 mm. As discussed in a previous section, the shorter pulse durations of the femtosecond lasers are expected to result in much shallower depth of compressive residual stresses. To reach the 0.1 mm depth of compressive stresses, a laser peening coverage of 2768% was utilized. These high coverages are possible due to the extremely high repetition rates (> 1 kHz) for femtosecond lasers. The fatigue testing data from the study showed a great increase in the fatigue life for the femtosecond laser peened samples. This new laser peening area has potential for applications where shallower residual stresses are sufficient and where typically used overlays are prohibitive or problematic.

9. Conclusion

It is an exciting time in the field of laser peening as technological advancements continue to greatly expand commercial applications for laser peening in ways that were not possible just a few years ago. Advancement in laser technology has reduced the cost, footprint and maintenance while improving the robustness of these systems to be incorporated in manufacturing production lines. Existing customers and new industry sectors will benefit from these advancements, resulting in safer, longer lasting components.

References

[1]   Anderholm NC. Laser-Generated Stress Waves. Appl Phys Lett 1970;16:113–5. https://doi.org/10.1063/1.1653116.

[2]   O'Keefe JD, Skeen CH. Laser-induced stress-wave and impulse augmentation. Appl Phys Lett 1972;21:464–6. https://doi.org/10.1063/1.1654220.

[3]   Fox JA, Barr DN. Laser-induced shock effects in Plexiglas and 6061-T6 aluminum. Appl Phys Lett 1973;22:594–6. https://doi.org/10.1063/1.1654520.

[4]   O'Keefe JD, Skeen CH, York CM. Laser-induced deformation modes in thin metal targets. J Appl Phys 1973;44:4622–6. https://doi.org/10.1063/1.1662012.

[5]   Fairand BP, Wilcox BA, Gallagher WJ, Williams DN. Laser shock-induced microstructural and mechanical property changes in 7075 aluminum. J Appl Phys 1972;43:3893–5. https://doi.org/10.1063/1.1661837.

[6]   Mallozzi P, Fairand B. Altering Material Properties. US3850698A, 1974.

[7]   Fairand BP, Clauer AH, Jung RG, Wilcox BA. Quantitative assessment of laser-induced stress waves generated at confined surfaces. Appl Phys Lett 1974;25:431–3. https://doi.org/10.1063/1.1655536.

[8]   Fairand BP, Clauer AH. Effect of water and paint coatings on the magnitude of laser-generated shocks. Opt Commun 1976;18:588–91. https://doi.org/10.1016/0030-4018(76)90327-8.

[9]   Clauer AH, Fairand BP, Wilcox BA. Pulsed laser induced deformation in an Fe-3 Wt Pct Si alloy. Metall Trans A 1977;8:119–25. https://doi.org/10.1007/BF02677273.

[10]   Fairand BP, Clauer AH. Laser generation of high-amplitude stress waves in materials. J Appl Phys 1979;50:1497–502. https://doi.org/10.1063/1.326137.

[11]   Clauer AH, Holbrook JH, Fairand BP. Effects of Laser Induced Shock Waves on Metals. Shock Waves High-Strain-Rate Phenom. Met., Boston, MA: Springer US; 1981, p. 675–702. https://doi.org/10.1007/978-1-4613-3219-0_38.

[12]   Clauer A., Walters C., Ford S. The Effects of Laser Shock Processing on the Fatigue Properties of 2024-T3 Aluminum. Lasers Mater. Process., Metals Park, OH, USA: ASM International; 1983, p. 7–22.

[13]   Clauer AH. Laser shock peening for fatigue resistance. In: Gregory JK., Rack HJ., Eylon

D., editors. Surf. Perform. Titan., Warrendale, PA: Minerals, Metals and Materials Society; 1996, p. 217–30.

[14] Fabbro R, Peyre P, Berthe L, Scherpereel X. Physics and applications of laser-shock processing. J Laser Appl 1998;10:265–79. https://doi.org/10.2351/1.521861.

[15] Fabbro R, Peyre P, Berthe L, Sollier A, Bartnicki E. Physics and applications of laser shock processing of materials. In: Chen X, Fujioka T, Matsunawa A, editors. High-Power Lasers Manuf., SPIE; 2000, p. 155. https://doi.org/10.1117/12.377012.

[16] Cowie W., Mannava S., Compton T. . Development of Laser Shock Peening of Airfoil Leading Edges For Single Engine Weapon Systems. USAF Aircr. Struct. Integr. Progr. Conf., San Antonio, TX: 1997.

[17] Sano Y., Mukai N., Aoki N., Konagai C. Laser Processing to Improve Residual Surface Stress of Metal Components. Dig. IEEE/Leos 1996 Summer Top. Meet., Keystone, CO: IEEE; 1996, p. 30–31.

[18] Clauer AH. Laser Shock Peening, the Path to Production. Metals (Basel) 2019;9:626. https://doi.org/10.3390/met9060626.

[19] Sano Y, Kimura M, Mukai N, Yoda M, Obata M, Ogisu T. Process and application of shock compression by nanosecond pulses of frequency-doubled Nd:YAG laser. In: Chen X, Fujioka T, Matsunawa A, editors. High Power Lasers Manuf., 2000, p. 294. https://doi.org/10.1117/12.377033.

[20] Kimura M., Sano Y;, Sudo A., Konagi C., Okano H., Shima S. Underwater Maintenance and Inspection Technology For Reactor Internals. 10th Pacific Basin Nucl. Conf., Kobe, Japan: Journal of Nuclear Science and Technolog; 1996, p. 518–25.

[21] Peyre P, Fabbro R, Berthe L, Scherpereel X, Bartnicki E. Laser-shock processing of materials and related measurements. In: Phipps CR, editor. High-Power Laser Ablation, Santa Fe, NM: SPIE; 1998, p. 183–93. https://doi.org/10.1117/12.321565.

[22] Peyre P, Merrien P, Lieurade RP, Fabbro R. Laser Induced Shock Waves As Surface Treatment For 7075–T7351 Aluminum Alloy. Surf Eng 1995;11:47–52. https://doi.org/10.1179/sur.1995.11.1.47.

[23] Procudo® Laser Peening System. LSP Technol Inc 2020:1–4. https://www.lsptechnologies.com/wp-content/uploads/2019/10/LSP_Technologies_Procudo_200b.pdf.

[24] Dane CB., Hackel LA., Daly J., Harrison J. Shot peening with lasers. Adv Mater Process 1998;153:37–8.

[25] Okazakie K., Ito A., Sano Y., Mukai N., Aoke N., Konagai C., et al. Underwater laser processing method and apparatus. US5790620A, 1996.

[26] Sano Y., Kimura M., Yoda M., Mukai N., Sato K., Uehara T., et al. Development of fiber-delivered laser peening system to prevent stress corrosion cracking of reactor components. 9th Int. Conf. Nucl. Eng., Nice, France: INIS; 2001.

[27] Toshiba. Changing Future of Manufacturing with Laser Peening 2019. https://www.toshiba-energy.com/en/nuclearenergy/topics/laserpeening.htm.

[28] Jialei Zhu, Xiangdong Jiao. Applications of underwater laser welding in nuclear power plant maintenance. 2011 Second Int. Conf. Mech. Autom. Control Eng., IEEE; 2011, p. 2947–50. https://doi.org/10.1109/MACE.2011.5987606.

[29] LSP Technologies' Portable Laser Peening System combats metal fatigue in hard-to-reach parts. LSP Technol Inc 2018. https://www.lsptechnologies.com/resources/lsp-technologies-portable-laser-peening-system-combats-metal-fatigue-in-hard-to-reach-parts/.

[30] Sano Y. Overview of Laser Peening without Sacrificial Overlay and Pioneering Novel Applications by Palmtop Lasers. 7th Int. Conf. Laser Peen. Relat. Phenom., Singapore: 2018.

[31] Malaki M, Ding H. A review of ultrasonic peening treatment. Mater Des 2015;87:1072–86. https://doi.org/10.1016/j.matdes.2015.08.102.

[32] Peyre P, Berthe L, Scherpereel X., Fabbro R. Laser-shock processing of aluminium-coated 55C1 steel in water-confinement regime, characterization and application to high-

cycle fatigue behaviour. J Mater Sci 1998;33:1421–1429.

[33] Hill MR. The Effects of Laser Peening on the Fatigue Behavior of Metallic Materials. First Int. Conf. Laser Peen., Houston, TX: 2008.

[34] Prevey P., Hornbach D., Mason P. Thermal Residual Stress Relaxation and Distortion in Surface Enhanced Gas Turbine Engine Components. 17th Heat Treat. Soc. Conf. First Int. Induction Heat Treat. Symp., Metals Park, OH, USA: ASM International; 1998, p. 3–12.

[35] Buchanan DJ, Shepard MJ, John R. Retained residual stress profiles in a laser shock-peened and shot-peened nickel base superalloy subject to thermal exposure. Int J Struct Integr 2011;2:34–41. https://doi.org/10.1108/17579861111108590.

[36] Shepard MJ., Smith PR., Prevey PS., Clauer AH. Thermal Stability of LSP Induced residual stresses in Ti-6Al-2Sn-4Zr-2Mo and IN100 Simulated Airfoil. 6th Natl. Turbine Engine High Cycle Fatigue Conf., Jacksonville, FL: Universal Technology Corporation; 2001.

[37] Telang A, Gill AS, Mannava SR, Qian D, Vasudevan VK. Effect of temperature on microstructure and residual stresses induced by surface treatments in Inconel 718 SPF. Surf Coatings Technol 2018;344:93–101. https://doi.org/10.1016/j.surfcoat.2018.02.094.

[38] Kattoura M, Mannava SR, Qian D, Vasudevan VK. Effect of laser shock peening on elevated temperature residual stress, microstructure and fatigue behavior of ATI 718Plus alloy. Int J Fatigue 2017;104:366–78. https://doi.org/10.1016/j.ijfatigue.2017.08.006.

[39] Thompson SD., See DW., Lykins CD., Sampson PG. A Preliminary Look at Laser Shock Peening to Improve Fatigue Life of Titanium 6Al-4V. In: Gregory JK;, Rack HJ., Eylon D., editors. Surf. Perform. Titan., Warrendale, PA: The Minerals, Metals & Materials Society; 1997, p. 239–51.

[40] Ruschau JJ, John R, Thompson SR, Nicholas T. Fatigue Crack Growth Rate Characteristics of Laser Shock Peened Ti-6Al-4V. J Eng Mater Technol 1999;121:321–9. https://doi.org/10.1115/1.2812381.

[41] Peyre P, Fabbro R, Merrien P, Lieurade HP. Laser shock processing of aluminium alloys. Application to high cycle fatigue behaviour. Mater Sci Eng A 1996;210:102–13. https://doi.org/10.1016/0921-5093(95)10084-9.

[42] Pistochini TE, Hill MR. Effect of laser peening on fatigue performance in 300M steel. Fatigue Fract Eng Mater Struct 2011;34:521–33. https://doi.org/10.1111/j.1460-2695.2010.01544.x.

[43] Clauer AH., Fairand BP., Slater JE. Laser shocking of 2024 and 7075 aluminum alloys. NASA-CR-145132, 1977.

[44] Peyre P, Scherpereel X, Berthe L, Fabbro R. Current trends in laser shock processing. Surf Eng 1998;14:377–80. https://doi.org/10.1179/sur.1998.14.5.377.

[45] Peyre P, Scherpereel X, Berthe L, Carboni C, Fabbro R, Béranger G, et al. Surface modifications induced in 316L steel by laser peening and shot-peening. Influence on pitting corrosion resistance. Mater Sci Eng A 2000;280:294–302. https://doi.org/10.1016/S0921-5093(99)00698-X.

[46] Fabbro R, Fournier J, Ballard P, Devaux D, Virmont J. Physical study of laser-produced plasma in confined geometry. J Appl Phys 1990;68:775–84. https://doi.org/10.1063/1.346783.

[47] Berthe L, Fabbro R, Peyre P, Tollier L, Bartnicki E. Shock waves from a water-confined laser-generated plasma. J Appl Phys 1997;82:2826–32. https://doi.org/10.1063/1.366113.

[48] Ballard P, Fournier J, Fabbro R, Frelat J. Residual Stresses Induced By Laser-Shocks. Le J Phys IV 1991;01:C3-487-C3-494. https://doi.org/10.1051/jp4:1991369.

[49] Forget P, Strudel JL, Jeandin M, Lu J, Castex L. Laser Shock Surface Treatment Of Ni-Based Superalloys. Mater Manuf Process 1990;5:501–28. https://doi.org/10.1080/10426919008953275.

[50] Pozdnyakov V, Oberrath J. 2D Simulations of the NS-Laser Shock Peening. 2019 IEEE Pulsed Power Plasma Sci., IEEE; 2019, p. 1–4. https://doi.org/10.1109/PPPS34859.2019.9009984.

[51] Meng X, Zhou J, Huang S, Su C, Sheng J. Properties of a Laser Shock Wave in Al-Cu

Alloy under Elevated Temperatures: A Molecular Dynamics Simulation Study. Materials (Basel) 2017;10:73. https://doi.org/10.3390/ma10010073.

[52] Li F, Qi X, Xiang D. Finite Element Modeling of Crack Generation in Laser Shock Peening Processed Airfoils. Adv Mater Sci Eng 2014;2014:1–10. https://doi.org/10.1155/2014/812705.

[53] Dupont V, Germann TC. Strain rate and orientation dependencies of the strength of single crystalline copper under compression. Phys Rev B 2012;86:134111. https://doi.org/10.1103/PhysRevB.86.134111.

[54] Wang Z, Beyerlein I, Lesar R. Plastic anisotropy in fcc single crystals in high rate deformation. Int J Plast 2009;25:26–48. https://doi.org/10.1016/j.ijplas.2008.01.006.

[55] Kattoura M. Multiscale Dislocation Dynamics Modeling of the High Strain Rate Deformation in Copper Single Crystal under Cyclic, Monotonic, & Shock Loading. American University of Beirut, 2013.

[56] Lainé SJ, Knowles KM, Doorbar PJ, Cutts RD, Rugg D. Microstructural characterisation of metallic shot peened and laser shock peened Ti–6Al–4V. Acta Mater 2017;123:350–61. https://doi.org/10.1016/j.actamat.2016.10.044.

[57] Kattoura M, Mannava SR, Qian D, Vasudevan VK. Effect of laser shock peening on residual stress, microstructure and fatigue behavior of ATI 718Plus alloy. Int J Fatigue 2017;102:121–34. https://doi.org/10.1016/j.ijfatigue.2017.04.016.

[58] Kim JH, Kim YJ, Kim JS. Effects of simulation parameters on residual stresses for laser shock peening finite element analysis. J Mech Sci Technol 2013;27:2025–34. https://doi.org/10.1007/s12206-012-1263-0.

[59] Frija M, Fathallah R, Hassine T. Finite Element Prediction of Laser Shock Peened Surface Modifications in Ti-6Al-4V Alloy. Key Eng Mater 2009;417–418:853–6. https://doi.org/10.4028/www.scientific.net/KEM.417-418.853.

[60] Amarchinta HK, Grandhi R V, Langer K, Stargel DS. Material model validation for laser shock peening process simulation. Model Simul Mater Sci Eng 2009;17:015010. https://doi.org/10.1088/0965-0393/17/1/015010.

[61] Sun R, Li L, Zhu Y, Zhang L, Guo W, Peng P, et al. Dynamic response and residual stress fields of Ti6Al4V alloy under shock wave induced by laser shock peening. Model Simul Mater Sci Eng 2017;25:065016. https://doi.org/10.1088/1361-651X/aa7a46.

[62] Li X, He W, Luo S, Nie X, Tian L, Feng X, et al. Simulation and Experimental Study on Residual Stress Distribution in Titanium Alloy Treated by Laser Shock Peening with Flat-Top and Gaussian Laser Beams. Materials (Basel) 2019;12:1343. https://doi.org/10.3390/ma12081343.

[63] Achintha M, Nowell D. Eigenstrain modelling of residual stresses generated by laser shock peening. J Mater Process Technol 2011;211:1091–101. https://doi.org/10.1016/j.jmatprotec.2011.01.011.

[64] Mura T. Micromechanics of defects in solids. 1st ed. Boston: Matrinus nijhoff; n.d.

[65] Prime MB, Hill MR. Measurement of Fiber-scale Residual Stress Variation in a Metal-matrix Composite. J Compos Mater 2004;38:2079–95. https://doi.org/10.1177/0021998304045584.

[66] Achintha M, Nowell D, Shapiro K, Withers PJ. Eigenstrain modelling of residual stress generated by arrays of laser shock peening shots and determination of the complete stress field using limited strain measurements. Surf Coatings Technol 2013;216:68–77. https://doi.org/10.1016/j.surfcoat.2012.11.027.

[67] FEA Modeling for Precision Laser Peening. LSP Technol Inc 2018. https://www.lsptechnologies.com/resources/fea-modeling-precision-laser-peening/ (accessed May 3, 2021).

[68] Munther M, Martin T, Tajyar A, Hackel L, Beheshti A, Davami K. Laser shock peening and its effects on microstructure and properties of additively manufactured metal alloys: a review. Eng Res Express 2020;2:022001. https://doi.org/10.1088/2631-8695/ab9b16.

[69] Kalentics N, de Seijas MOV, Griffiths S, Leinenbach C, Logé RE. 3D laser shock peening – A new method for improving fatigue properties of selective laser melted parts.

Addit Manuf 2020;33:101112. https://doi.org/10.1016/j.addma.2020.101112.

[70] Laser Peen Forming. LSP Technol Inc 2018. https://www.lsptechnologies.com/laser-solutions/laser-peen-forming/ (accessed March 3, 2020).

[71] Yocom CJ, Zhang X, Liao Y. Research and development status of laser peen forming: A review. Opt Laser Technol 2018;108:32–45. https://doi.org/10.1016/j.optlastec.2018.06.032.

[72] Lubatschowski H. Applications of the Femtosecond Laser 2012. https://crstodayeurope.com/articles/2012-feb/applications-of-the-femtosecond-laser/#:~:text=Useful features of femtosecond lasers,%2C CXL%2C and reversing cataract. (accessed May 3, 2021).

[73] Femtosecond Laser. ScienceDirect 2015. https://www.sciencedirect.com/topics/engineering/femtosecond-laser (accessed May 3, 2021).

[74] Sano T, Eimura T, Kashiwabara R, Matsuda T, Isshiki Y, Hirose A. Femtosecond laser peening of 2024 aluminum alloy without a sacrificial overlay under atmospheric conditions. J Laser Appl 2017;29:012005. https://doi.org/10.2351/1.4967013.